Earth and Planetary Science Letters 331-332 (2012) 67–79

Contents lists available at SciVerse ScienceDirect

Earth and Planetary Science Letters

journal homepage: www.elsevier.com/locate/epsl

Earth at 200 Ma: Global palaeogeography refined from CAMP palaeomagnetic data

Vicente Carlos Ruiz-Martínez [a,b,*], Trond H. Torsvik [b,c,d,e], Douwe J.J. van Hinsbergen [b,c], Carmen Gaina [b,c]

[a] Departamento de Geofísica y Meteorología, Facultad de Física, Universidad Complutense de Madrid, Avda. Complutense s/n, 28040 Madrid, Spain
[b] Center for Physics of Geological Processes, University of Oslo, 0316 Oslo, Norway
[c] Center of Advanced Study, Norwegian Academy of Science and Letters, 0271 Oslo, Norway
[d] Geodynamics, NGU, N-7491 Trondheim, Norway
[e] School of Geosciences, University of the Witwatersrand, WITS, 2050, South Africa

ARTICLE INFO

Article history:
Received 21 November 2011
Received in revised form 26 January 2012
Accepted 2 March 2012
Available online xxxx

Editor: P. DeMenocal

Keywords:
palaeomagnetism
palaeogeography
Pangea breakup
mantle plumes
CAMP
Morocco

ABSTRACT

The Central Atlantic Magmatic Province was formed approximately 200 Ma ago as a prelude to the breakup of Pangea, and may have been a cause of the Triassic–Jurassic mass extinction. Based on a combination of (i) a new palaeomagnetic pole from the CAMP related Argana lavas (Moroccan Meseta Block), (ii) a global compilation of 190–210 Ma poles, and (iii) a re-evaluation of relative fits between NW Africa, the Moroccan Meseta Block and Iberia, we calculate a new global 200 Ma pole (latitude = 70.1° S, longitude = 56.7° E and A_{95} = 2.7°; N = 40 poles; NW Africa co-ordinates). We consider the palaeomagnetic database to be robust at 200 ± 10 Ma, which allows us to craft precise reconstructions near the Triassic–Jurassic boundary: at this very important time in Earth history, Pangea was near-equatorially centered, the western sector was dominated by plate convergence and subduction, while in the eastern sector, the Palaeotethys oceanic domain was almost consumed because of a widening Neothethys. We show that there has been negligible net displacement of the Moroccan Meseta relative to Africa since 200 Ma. We calculate a new fit between Iberia and NW Africa, showing that models inferring minor Cretaceous rotation and major Cretaceous sinistral translation of Iberia relative to Europe are inconsistent with palaeomagnetic Iberia–Africa fits at 200 Ma. During Pangea breakup (~195 Ma, opening of the Central Atlantic), and shortly after the CAMP outburst, Laurasia rotated clockwise relative to Gondwana around an Euler pole located in SE Iberia. The CAMP and its likely contribution to climate change, mass extinction and Pangea breakup profoundly changed planet Earth and we show that CAMP was sourced by a deep mantle plume that started its disturbing journey from the core–mantle boundary.

1. Introduction

Almost 100 years ago, Alfred Wegener (1915) proposed that all continents once formed a single supercontinent, named Pangea, surrounded by the vast marine area of the Panthalassa Ocean. His Pangea reconstruction was partly based on the similarity in South Atlantic coastlines, but he also pointed out that Permian and Carboniferous plant and animal fossils from a number of continents, now separated by the Atlantic and Indian Oceans, were largely identical. Based on the distribution of glacial deposits, he was convinced that a continental ice cap must have covered the contiguous southern parts of Pangea in the late Carboniferous. If we compare Wegener's Pangea with modern reconstructions, which are based on a much larger database and more disciplines, there are many similarities, but the most striking difference is its palaeolatitude location due to our modern knowledge on palaeomagnetic data. We can therefore directly study how climate-sensitive (latitude-dependent) sedimentary rock facies have been distributed across the Earth's surface (e.g., Torsvik and Cocks, 2004). Moreover, novel techniques using the distribution of large igneous provinces and kimberlites (Burke and Torsvik, 2004; Torsvik et al., 2008b, 2010), and their relationship to the so-called plume-generation zones at the core–mantle boundary (Burke et al., 2008), as well as fitting former active margins to subducted slab remnants in the lower mantle (van der Meer et al., 2010), all allow now, for the first time, to also determine the palaeolongitude of Pangea, by a direct comparison of the mantle to the surface of the Earth.

Pangea did not include all continents at any given time – it reached its maximum size during late Palaeozoic and early Mesozoic times – but the most important growth phase occurred during the late Carboniferous when Gondwana, Laurussia and intervening terranes collided, and in the process produced the Alleghenian–Hercynian Orogenic Belt (Matte, 2001; Torsvik and Cocks, 2004). Already by mid-Permian times (~265 Ma) many former peri-Gondwana terranes (darker shaded green in Fig. 1a) started to separate from the NE Gondwana margin, opening the Neotethys in its wake (e.g., Şengör et al., 1984; Stampfli and Borel, 2002).

One of the most important phases of the breakup of Pangea started at around 200 Ma, when the central Atlantic Ocean began to form (Labails et al., 2010; Sahabi et al., 2004). Probably not coincidentally

* Corresponding author.
E-mail address: vcarlos@fis.ucm.es (V.C. Ruiz-Martínez).

0012-821X/$ – see front matter © 2012 Elsevier B.V. All rights reserved.
doi:10.1016/j.epsl.2012.03.008

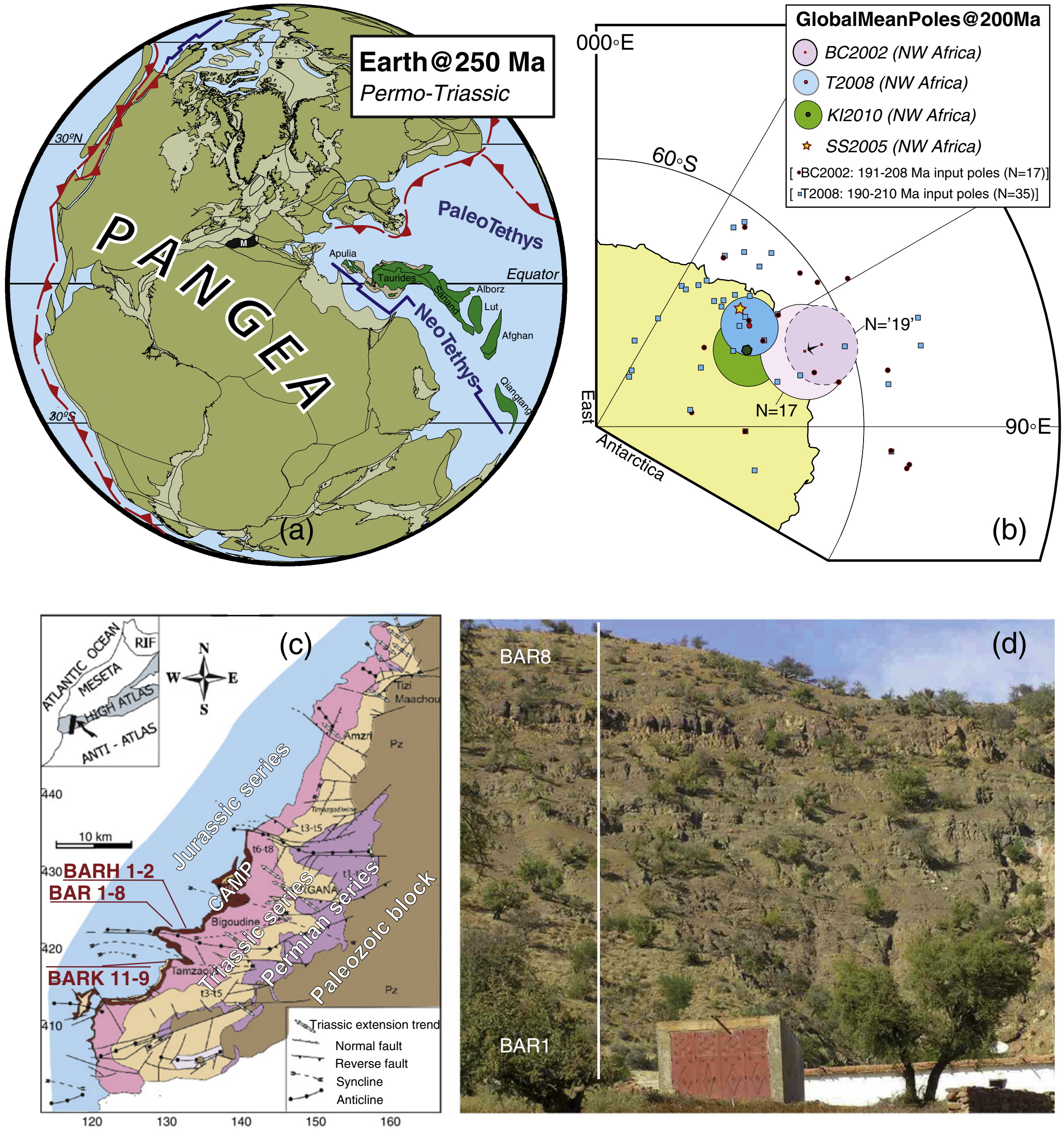

Fig. 1. (a) Pangea reconstruction at 250 Ma. At this time the Neotethys ocean is opened; former peri-Gondwana terranes that include the Taurides, Sanand, Albortz, Lut, Afghan and the Tibetan Qiangtang Terrane are shown in darker green (after Cocks and Torsvik, 2011; Torsvik and Cocks, 2004; Torsvik et al., in review). The Moroccan Meseta block in northern Africa is shaded in black and denoted as M. Active subduction is shown by red lines and active sea floor spreading by blue segments. This reconstruction uses a mean 250 Ma palaeomagnetic pole of 45.8° S and 57.8° E ($A_{95}=3.6°$) in NW African co-ordinates (calculated from Torsvik et al., in review). Relative fits are listed in Table 4; (b) Comparison of the original global mean 200 Ma poles of Besse and Courtillot (2002, pink A_{95}s) and Torsvik et al. (2008a, blue A_{95}s). Lighter pink A_{95}s are the mean pole of Besse and Courtillot (2002) using plate circuits of Torsvik et al. (2008a). Note that two input poles were duplicated in the Besse and Courtillot (2002) analysis and our analysis is based on their 17 poles and not N = 19 as stated in their paper. This does not change their mean pole significantly but A_{95} becomes larger. Input poles for both models are shown with Torsvik et al. (2008a) plate circuits. Note that all mean/individual poles are shown in NW Africa co-ordinates. We also plot the 200 Ma mean pole of Schettino and Scotese (2005) as a yellow star (no error estimate for their mean pole), and the 200 Ma mean pole of Kent and Irving (2010); the latter is based on only seven global poles but almost identical to that of Torsvik et al. (2008a); (c) structural map of the Argana Basin and location of CAMP sampled sections (modified from Frizon de Lamotte et al., 2008; Medina, 1991); (d) BAR1 to BAR8 lava flow sequence. (For interpretation of the references to color in this figure legend, the reader is referred to the web version of this article.)

(e.g. Burke and Dewey, 1973; Courtillot et al., 1999), the region of central Atlantic breakup was around the same time affected by the emplacement of the Central Atlantic Magmatic Province (CAMP) — one of the largest flood basalt provinces in the world (Marzoli et al., 1999). Not only did CAMP emplacement form the prelude of the main dismemberment of Pangea, it also had a profound climatic effect, with many authors supporting a direct link between CAMP and the end-Triassic mass extinction (e.g., Deenen et al., 2010; Hesselbo et al., 2002; Ruhl et al., 2010; Whiteside et al., 2010).

In this paper, we document new palaeomagnetic data from CAMP lavas in Morocco (part of the Moroccan Meseta block in Fig. 1a, c), and review the palaeomagnetic database to improve the palaeomagnetic constraints (for Africa specifically and on the global plate circuit in general), provide latitude- and longitude-constrained positions for the plate circuit, and show the latest state of the art in palaeogeography. This will provide a context and basis for future interdisciplinary research on the dramatic changes in Earth history at the onset of the Jurassic, some 200 Ma ago.

2. Existing palaeomagnetic mean poles at 200 Ma

Palaeomagnetic reconstructions are conveniently expressed in terms of Apparent Polar Wander Paths (APWPs). Taking relative plate motions constrained by ocean floor geophysical data into account, palaeomagnetic data from all continents can be combined to a global APWP (GAPWaP). Two widely used GAPWaPs are those of Besse and Courtillot (2002) and Torsvik et al. (2008a). For the last 200 Ma these two paths differ by only 3.9 ± 3.3° on average (great-circle distance – GCD – between mean poles of the same age ± standard deviation), but the largest difference (~11°) is seen at 200 Ma, the moment of focus of this paper. This may originate from different data selection, different plate circuits, differences in intraplate deformation reconstructions, or a combination of these causes. In terms of data-selection, Besse and Courtillot (2002) included 17 poles from four plates (none from Africa) while Torsvik et al. (2008a) included 35 poles (190–210 Ma) from eight plates including Africa. Global mean poles at 200 Ma are statistically different (Fig. 1b), but by using Torsvik et al.'s (2008a) plate circuits with the poles selected by Besse and Courtillot (2002), the 200 Ma mean poles statistically overlap with GCD reduced to 6.8°. About 50% of the difference at 200 Ma can therefore result from the difference in plate circuits; as an example, Torsvik et al. (2008a) use tighter fits between North America and NW Africa and North America vs. Europe in order to account for pre-breakup extension.

An alternative APWP was published by Schettino and Scotese (2005), who arrived at a GAPWaP that shows gross similarities with that of Besse and Courtillot (2002) and Torsvik et al. (2008a) for the past 100 Ma. Schettino and Scotese (2005) spline-filtered their input poles while analyzing inclination and declination data separately; however, the appropriate method is to fit spherical splines directly to the palaeopoles since this smoothing approach is independent of the position on the globe. Nevertheless, the Schettino and Scotese (2005) mean 200 Ma pole (yellow star in Fig. 1b) compares favorably with that of Torsvik et al. (2008a) despite different data selection, plate circuits and analytical approach. Similarly, a recent 200 Ma mean pole of Kent and Irving (2010, Fig. 1b), based on only seven input poles after strict filtering of the global data (and excluding all sedimentary poles not corrected for inclination shallowing) yields a mean pole that is practically identical (GCD = 2.8°) to that of Torsvik et al. (2008a).

In recent years, palaeomagnetic information that has been published from igneous rocks of the CAMP has not been taken into account in computing the existing GAPWaPs. We review these data, provide new palaeomagnetic data from CAMP lavas in Morocco, and use the new combined dataset to recalculate a new 200 Ma mean pole. A specific complexity in using northwest African poles results from claims that the Meseta block of NW Morocco, from which part of the palaeomagnetic constraints on the 200 Ma APWP was derived, has undergone motion with respect to Africa (e.g., Labails et al., 2010; Sahabi et al., 2004; Schettino and Turco, 2009). We will re-assess the arguments for this inferred mobility and the corrections that were proposed.

3. Geological setting and the tectonic stability of the Moroccan Meseta

Morocco comprises continental crust in the northwest that remained essentially undeformed since the Mesozoic – the Moroccan Meseta Block – separated from the stable African continent by the Cenozoic High Atlas mountain belt. CAMP-related intrusives and lavas are widespread in Morocco and below we present new data from CAMP lavas in the Argana basin, positioned at the southeastern margin of the Moroccan Meseta Block at the boundary of the High Atlas Mountains (Fig. 1c).

Although classic plate reconstructions of the Central Atlantic assumed rigidity of northwest Africa (e.g., Klitgord and Schouten, 1986), several authors have suggested that the Moroccan Meseta should be treated as a mobile block during the evolution of the Central Atlantic, disconnected from Africa across the High Atlas mountain belt (Labails et al., 2010; Sahabi et al., 2004). The geological record provides support for some mobility of the Moroccan Meseta relative to Africa. The Atlas Mountains comprise Mesozoic sediments, which were deposited in an intracontinental rift zone that cut through upper Palaeozoic and older basement and became inverted during Cretaceous–Cenozoic Africa–Iberia convergence (Frizon de Lamotte et al., 2008). Sahabi et al. (2004) applied a net post-200 Ma clockwise rotation of the Moroccan Meseta block, suggesting a north(east)ward increasing shortening of the High and Middle Atlas of up to ~100 km in the north(east), and approximately 50–60 km in the Central High Atlas. Alternatively, Schettino and Turco (2009) postulated that Jurassic Atlantic spreading, interpreted by most authors to be mainly accommodated between Iberia and Africa (e.g., Dewey et al., 1989), was for a significant part partitioned into the Atlas rift system,

Table 1
ChRM site-mean directions and VGPs from Argana lava flows after (*before) bedding correction. Section names follow Aït Chayeb et al. (1998). SLat/SLon, site latitude/longitude; Dip Az/Dip, dip azimuth/dip of the section/lava-flow; n′/n, number of analyzed samples/included in site–mean determinations (gc, great circle determination); Dec/Inc, declination/inclination; k/α_{95}/R, precision parameter/95% confidence circle/resultant vector length; PLat/PLon, VGP latitude/longitude; Palat, palaeolatitude.

Section, site	SLat	SLon	Dip Az	Dip	n′	n	Dec*	Inc*	Dec	Inc	k	α_{95}	R	PLat	PLon	Palat
Tasguint																
BAR1	30.73	−9.24	6	19	8	8	354.6	55.9	358.0	37.1	293	3.2	7.98	−79.8	1.4	20.7
BAR2	30.73	−9.24	6	19	8	6	340.9	54.6	348.1	36.9	63	8.5	5.92	−75.2	40.1	20.6
BAR3	30.73	−9.24	6	19	8	7	323.6	59.2	337.6	43.6	250	3.8	6.98	−69.6	71.4	25.5
BAR4	30.73	−9.24	6	19	9	7	323.5	57.0	336.5	41.4	174	4.6	6.97	−68.0	68.1	23.8
BAR5	30.73	−9.24	6	19	8	8	312.1	50.0	325.5	36.9	86	6.0	7.92	−57.4	70.9	20.6
BAR6	30.73	−9.24	6	19	8	8	308.8	50.6	323.2	38.2	380	2.8	7.98	−55.9	74.0	21.5
BAR7	30.73	−9.24	6	19	8	8	320.1	52.3	332.4	37.6	96	5.7	7.93	−63.4	66.0	21.1
BAR8	30.73	−9.24	6	19	8	7	329.4	57.6	340.9	41.2	320	3.4	6.98	−71.6	62.7	23.6
Alemzi North																
BARh1	30.73	−9.25	21	26	8	7	346.9	45.5	355.8	22.8	116	5.6	6.95	−70.7	3.3	11.9
BARh2	30.73	−9.25	21	26	8	7	326.1	51.1	343.4	32.8	67	7.4	6.91	−70.2	44.1	17.9
Imerhrame																
BARk11	30.69	−9.26	302	34	9	6 (gc)	5.5	42.3	347.5	22.0	133	7.6	5.99	−67.5	24.4	11.4
BARk10	30.69	−9.27	310	27	9	7 (gc)	12.2	60.0	346.3	41.8	156	5.9	6.98	−76.2	55.5	24.1
BARk9	30.69	−9.27	310	27	8	7	331.6	57.8	323.4	31.9	118	5.6	6.95	−54.2	67.3	17.3

		N	Dec	Inc	k	α_{95}	R	PLat	PLon	K	A_{95}	R
ARG flows	Bedding corrected	13	340.1	36.2	49	6.0	12.76	−69.2	55.5	48	6.0	12.75
	No correction	13	334.9	54.9	40	6.6	12.70	−68.4	100.9	23	8.8	12.48

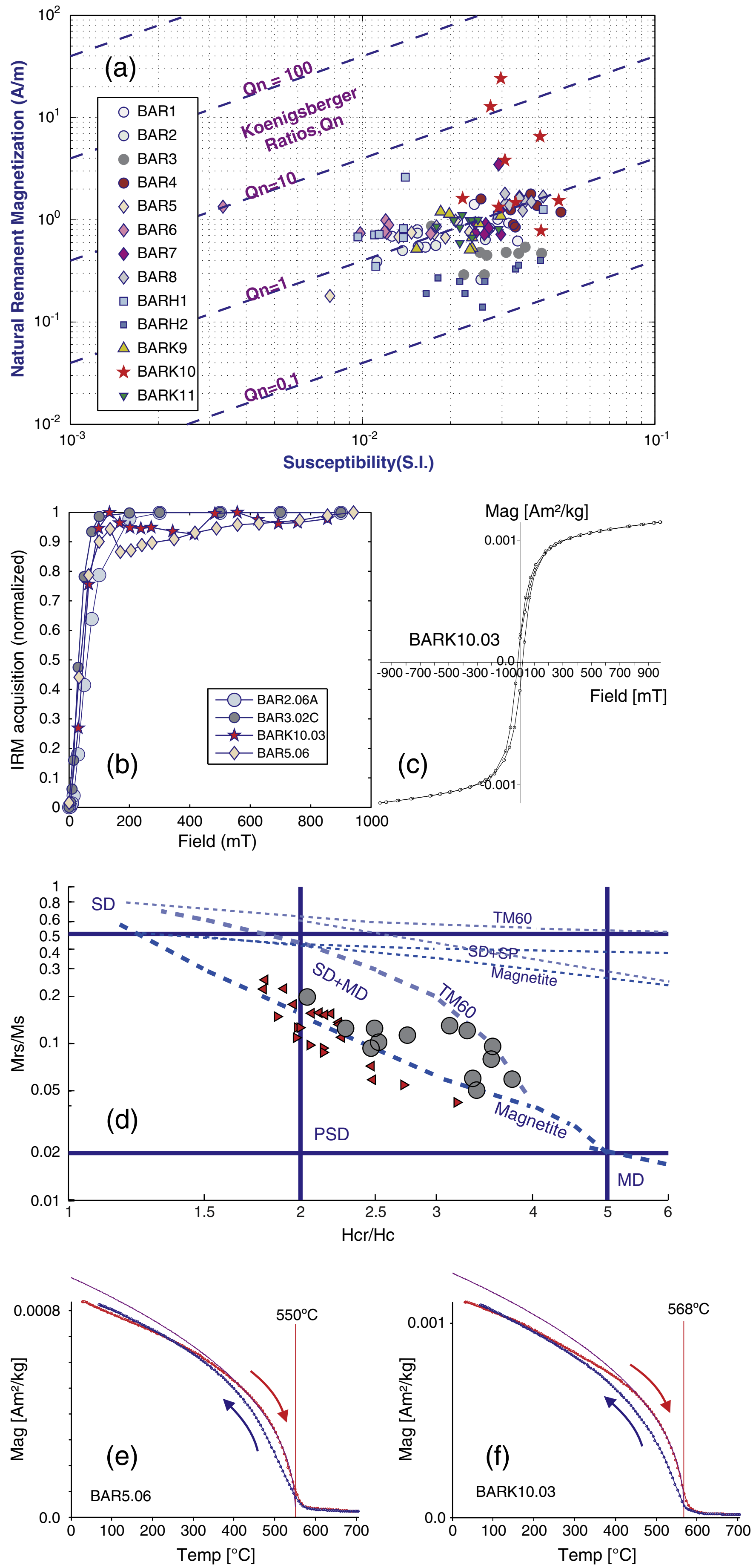

(a)
Natural Remanent Magnetization (A/m)
Susceptibility(S.I.)
Qn = 100
Koenigsberger Ratios,Qn
Qn=10
Qn=1
Qn=0.1
BAR1
BAR2
BAR3
BAR4
BAR5
BAR6
BAR7
BAR8
BARH1
BARH2
BARK9
BARK10
BARK11
(b)
IRM acquisition (normalized)
Field (mT)
BAR2.06A
BAR3.02C
BARK10.03
BAR5.06
(c)
Mag [Am²/kg]
BARK10.03
Field [mT]
(d)
Mrs/Ms
Hcr/Hc
SD
TM60
SD+SP
Magnetite
SD+MD
PSD
MD
(e)
Mag [Am²/kg]
550°C
BAR5.06
Temp [°C]
(f)
568°C
BARK10.03

leading to up to 170 km of dextral offset during the Mesozoic, a view that was recently challenged (Labails and Roest, 2010). Nevertheless, it is important to take this discussion into account when we use our new results to constrain a 200 Ma pole for the GAPWaP.

The Atlas mountains are subdivided into an Atlantic domain (formed by the Western High Atlas and the Atlantic Margin) and a Tethyan domain (formed by the Central and Eastern High Atlas and the Middle Atlas) (see Frizon de Lamotte et al., 2008 for a comprehensive review of this region). Extension in the Atlantic domain mainly occurred prior to the deposition of the ~200 Ma CAMP lavas, which filled the extensional basins and are found at the base of a lower Liassic evaporite-filled sag basin (Frizon de Lamotte et al., 2008). However, in the central and eastern Atlas, the middle Atlas and the Saharan Atlas of Algeria, extension continued into the Jurassic (up to ~160 Ma; Beauchamp et al., 1999). The intracontinental Atlas rift became inverted as a result of Cretaceous and younger plate convergence between Africa and Europe and uplift dominantly occurred between 30 and 20 Ma (Beauchamp et al., 1999). Shortening estimates for the Atlas mountains are based on balancing of structural cross-sections across the High Atlas, using seismic profiles and geological mapping. Early estimates of Brede (1992) suggested shortening percentages on the order of 10–20% (~10–20 km) across the High Atlas. Beauchamp et al. (1999) provided the highest estimates of at least 36 km of High Atlas shortening, and reconstructed an original width of the Atlas rift of 113 km, comparable to the Red Sea. However, later shortening estimates (Arboleya et al., 2004; Teixell et al., 2003) for three cross-sections across the High Atlas also suggested less shortening, of only 13–30 km. In the Middle Atlas, shortening is Tortonian and younger, and minimal (~5 km, Arboleya et al., 2004; Gomez et al., 1998).

We note that these shortening values are at least ~50% less than suggested for this region by the Euler poles for the Moroccan Meseta of Sahabi et al. (2004). Moreover, reconstruction back to 200 Ma should not only correct for post-Cretaceous shortening of the Atlas, but also for Jurassic extension of the Atlas rift. The total amount of Jurassic extension is not precisely constrained, but is probably on the order of few tens of km, given the total original rift width of ~110 km (Beauchamp et al., 1999). In any case, the net shortening since 200 Ma must be less than the 13–36 km of shortening that comes from balanced cross-sections. Hence, there seems to be no structural geological basis to infer significantly deviating motion of the Moroccan Meseta from Africa. In this paper we will test a Sahabi et al. (2004) scenario, as well as a scenario in which the Moroccan Meseta did not undergo a net motion with respect to Africa after 200 Ma.

4. New palaeomagnetic data at 200 Ma

4.1. Sampling

New palaeomagnetic data come from the ~200 Ma Central Atlantic Magmatic Province (CAMP, Fig. 1c, d) tholeiitic basaltic lava sequence in the Argana basin, Morocco. The NE–SW trending Argana basin (Fig. 1c) is located between Agadir and Marrakech, in the western High Atlas, within the Moroccan Meseta province. With local exceptions near major faults, CAMP-related sediments strike roughly parallel with the trend of the basin and dip 5–20° toward the west (Brown, 1980). The basaltic sequence consists of two main units separated by a metric-scaled sedimentary level or palaeosol, the so-called Tasguint (~60 m thick at the base) and Alemzi (~140 m thick at the top) Formations, which are correlated along many sections throughout the basin (Aït Chayeb et al., 1998; El Hachimi et al., 2011). Sampling was performed in 13 sites from three sections (Fig. 1c) with slightly different bedding attitudes (Table 1). Lava attitudes were measured as the average of several estimates of strike and dip directions of both the basalts and the surrounding (host or intra-lava) sedimentary layers, and orthogonal solutions of the columnar disjunction planes when available. At each site, eight to nine cores (Table 1) were sampled in fresh, massive cores of layered lavas, except at site BARK10 where basalts displayed prismatic jointing. From bottom to top in each of the three sampled sections, (1) sites BAR1 to BAR8 (Fig. 1d) correspond to successive, 5–10 m thick lavas covering the ~80 m thick "Tasguint" section; (2) sites BARH1 and BARH2 are consecutive lavas separated by a thin sedimentary horizon within the "Alemzi North" section; and (3) sites BARK11 (overlain by a reddish sedimentary layer), BARK10 and BARK9 (close to the top, host sediments), ~20 m apart, belong to the "Imerhrane" section (see "*f*", "*g*", "*c*" and "*III*", "*IV*" lithostratigraphic columns in Aït Chayeb et al., 1998 and El Hachimi et al., 2011, respectively).

4.2. Age constraints

K–Ar ages of Argana basin CAMP lavas from the late 1970s yielded ages of 197 ± 17 Ma (Manspeizer et al., 1978), 207 ± 8 Ma and 205 ± 12 Ma (Westphal et al., 1979). More recently, Verati et al. (2007) reported $^{40}Ar/^{39}Ar$ ages from Moroccan CAMP samples from the central High Atlas and Oujda basins (an Argana sample yielded no plateau age), ranging from 197.8 ± 0.7 Ma to 201.7 ± 2.4 Ma with a restricted peak at 199.1 ± 1 Ma. Moroccan results agree with abundant African CAMP $^{40}Ar/^{39}Ar$ data clustering at 199 Ma (e.g., Nomade et al., 2007), with uncertainties of 1–2 Ma on individual dates. A short duration for the peak CAMP activity of less than 1 Ma has been suggested (Knight et al., 2004; Marzoli et al., 2004). Milankovitch cyclostratigraphic estimates at the eastern North America extensional rifts constrain the duration of the corresponding CAMP event to ~600 ky (Olsen et al., 2003; Whiteside et al., 2007). Whiteside et al. (2007) argued for time correlation between homotaxial (Olsen et al., 2003), CAMP-bearing strata of eastern North America (especially the Fundy basin, Nova Scotia) and western Morocco (Argana and Central High Atlas basins). Schoene et al. (2006, 2010) reported high precision $^{206}Pb/^{238}U$ zircon CAMP data of 201.27 ± 0.27 Ma and 201.38 ± 0.31 Ma at the North Mountain Basalt (Fundy basin). Deenen et al. (2010) suggested that the lowermost CAMP lavas of Argana are ca. 20 ka older than the Orange Mountain basalts of Newark basin. At the Moroccan CAMP lavas from the High Atlas, Knight et al. (2004) identified at least one short reversed chron between normal polarities in the volcanic pile, subsequently used in trans-Atlantic CAMP correlations. Font et al. (2011) revisited this magnetostratigraphy pointing to a remagnetization affecting the interbedded limestones, which registered the Knight et al. (2004) reversal, and normal polarities in other correlated lava sections from the High Atlas. Preliminary palaeomagnetic (Ruiz-Martínez et al., 2007; Westphal et al., 1979) and recent magnetostratigraphic results (Deenen et al., 2011a) from the Argana basin identified only normal polarities in CAMP-related lavas. The available age constraints thus constrain a 201 Ma age for the sampled rocks.

4.3. Rock magnetism

Low field magnetic susceptibility (χ) was measured on an AGICO KLY-3 susceptibility bridge. The natural remanent magnetization (NRM) and isothermal remanent magnetization (IRM) were measured on a 2 G cryogenic magnetometer (model 755 DC SQUID) and an AGICO JR5-A spinner magnetometer at the Universities of Burgos (UBU) and Madrid (UCM). NRM intensity and χ values are shown in Fig. 2a together with

Fig. 2. Representative rock magnetic results from the Argana basaltic flows: (a) Koenigsberger ratio, Q_n; (b) IRM acquisition curves; (c) hysteresis loop (before the paramagnetic contribution correction); (d) hysteresis parameter ratios of representative samples of all sampled flows (big circles) are compared with those obtained from Moroccan CAMP intrusives [IG and FZ dykes (left and right triangles); Palencia-Ortas et al., 2011], along with characteristic trends (Dunlop, 2002) for mixtures of single domain (SD) and multidomain (MD) [or superparamagnetic (SP)] magnetite and 60% Ti-titanomagnetite (TM60) grains; and (e, f) thermomagnetic curves from two different sections indicating Curie-temperatures of 550 and 568 °C. In both examples, heating (red) and cooling (blue) curves are almost reversible. (For interpretation of the references to color in this figure legend, the reader is referred to the web version of this article.)

calculated remanent/induced magnetization ratios, Q_n (Koenigsberger values). Those specimens with both high Q_n values and NRM intensities come from the BARK10 site (Fig. 2a), suggesting the potential presence of a lightning induced IRM. The remaining samples have NRM intensities, χ and Q_n values typical of thermoremanent magnetizations in pristine basaltic rocks. IRM was imparted in representative specimens using an ASC Scientific IM10-30 impulse magnetizer and in rock chips using a Variable Field Translation Balance (MM VFTB). Despite a slightly noisy signal in the latter, IRM acquisition curves are dominated by low coercivity (<0.2 T) minerals (Fig. 2b). The MM VFTB was also used to perform back-field curves, hysteresis loops and thermomagnetic measurements. Closed pot-bellied hysteresis loops, saturation of the ferromagnetic grains and little or no paramagnetic/diamagnetic high field contributions were observed (Fig. 2c). Corrected ferromagnetic hysteresis parameters fall in domain state boundaries (Fig. 2d) consistent with single and multi-domain mixture of magnetite or low-Ti titanomagnetite (Dunlop, 2002). This is also supported by Curie-temperature determinations, which are slightly lower but often close (Fig. 2e, f) to that of pure magnetite. Thermomagnetic curves are almost reversible.

4.4. Demagnetization behavior

Thermal (TH) and alternating field (AF) demagnetizations were first carried out for pilot specimens from the same sample at each site, in 12 to 14 steps up to temperatures and peak fields of 600 °C and 130 mT (Fig. 3a, b). Demagnetization was performed with a TD48-SC (ASC) thermal demagnetizer and the automatic 2G AF demagnetization unit. Two remanence components are readily identified: a low unblocking temperature (320 °C) or low-medium coercivity (10–40 mT) component, and a second component isolated above 370–575 °C or from 20–45 mT to 90–130 mT. The first component is considered a viscous remagnetization because the directions plot close to the present-day field (albeit scattered). The high unblocking temperature/coercivity components are characterized by north-westerly declinations and positive inclinations (Fig. 3a–c), and interpreted as the characteristic remanent component of magnetization (ChRM). Moroccan CAMP-related Central High Atlas lava flows also exhibited these two magnetic components with similar thermal and AF spectra ranges (Knight et al., 2004). Based on the magnetic behavior of the pilot samples we used AF

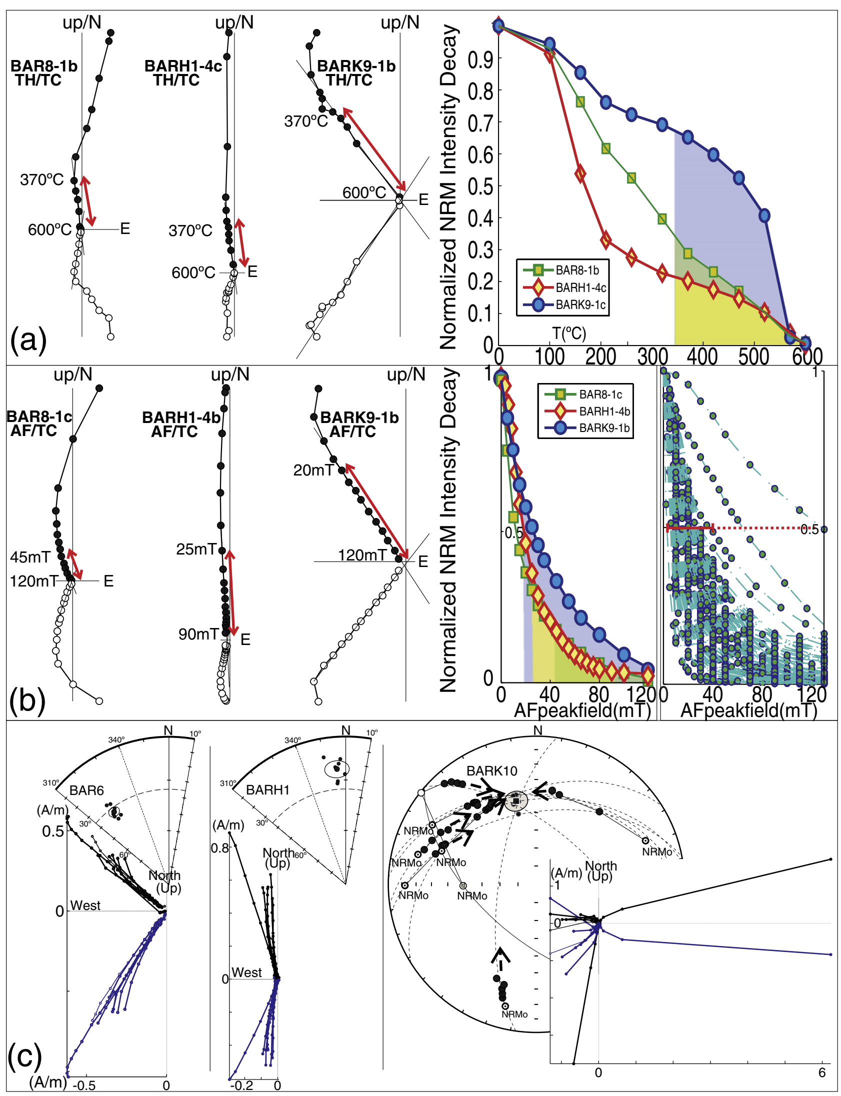

Fig. 3. Characteristic examples of thermal (a) and AF (b) demagnetization paths (all bedding corrected) of twin specimens from the three sampled sections together with the corresponding normalized intensity decay plots. Numbers linked by arrows in orthogonal plots (and shadowed areas below decay plots) refer to temperature and AF intervals used to calculate the ChRM. In orthogonal vector-plots, open (solid) symbols represent projections onto the vertical (horizontal) planes, respectively. AF decay plots (*right hand* diagram) show median destructive fields of 5–40 mT. (c) Equal area plots show ChRMs and calculated site-mean directions (after bedding correction) with α_{95} confidence circles for representative sites from the Tasguint (BAR6), Alemzi North (BARH1) and Imerhrame (BARK10, mean direction calculated from great-circle intersections) sections. Orthogonal vector plots (only AF demagnetizations paths) are shown before bedding correction. Black (blue) lines denote horizontal (vertical) plane projections. (For interpretation of the references to color in this figure legend, the reader is referred to the web version of this article.)

demagnetization to estimate the ChRMs of the remaining samples, which were fully demagnetized in ten steps up to 130 mT (10 mT steps up to 50 mT and then 20 mT steps up to 130 mT). The median destructive fields ranged between 5 and 40 mT (Fig. 3b, right-hand diagram). Because of overlapping coercivity spectra in samples from two sites (BARK10, BARK11), the AF technique did not lead to stable linear end-points but to planes defined by the viscous (?) remagnetizations and the potentially primary ChRM directions (Fig. 3c, right-hand diagram), great circles converging in the (relatively less scattered) ChRM direction. Principal component analysis (Kirschvink, 1980) was used to estimate the directions of lines and planes of best least-squares fit along the AF demagnetization path of the analyzed specimens, with a minimum of six demagnetization steps involved (Fig. 3c, "additional figure" in Supplementary material).

4.5. A new 200 Ma palaeopole from the Moroccan Meseta Province

ChRMs from the Argana basalts are all of normal polarity (Fig. 4). The palaeomagnetic data are usually of excellent quality (Fig. 3), but when computing site-mean directions, those demagnetization fits with maximum angular deviations (Kirschvink, 1980) greater than 5° (rare) were excluded. A few samples with high NRM intensities, and related to higher Q_n values (>10), were also not included (see n′ vs. n in Table 1). Fisher statistics (Fisher, 1953) were used to compute site-mean directions and palaeomagnetic poles for the Argana lavas (Table 1). At each site, ChRM directions pass Fisherian distribution tests, the data are well-clustered ($\alpha_{95} \leq 8.5°$), all sites yield k values > 50, which is commonly used (e.g., Deenen et al., 2011b; Johnson et al., 2008) as a minimum value for a reliable lava site.

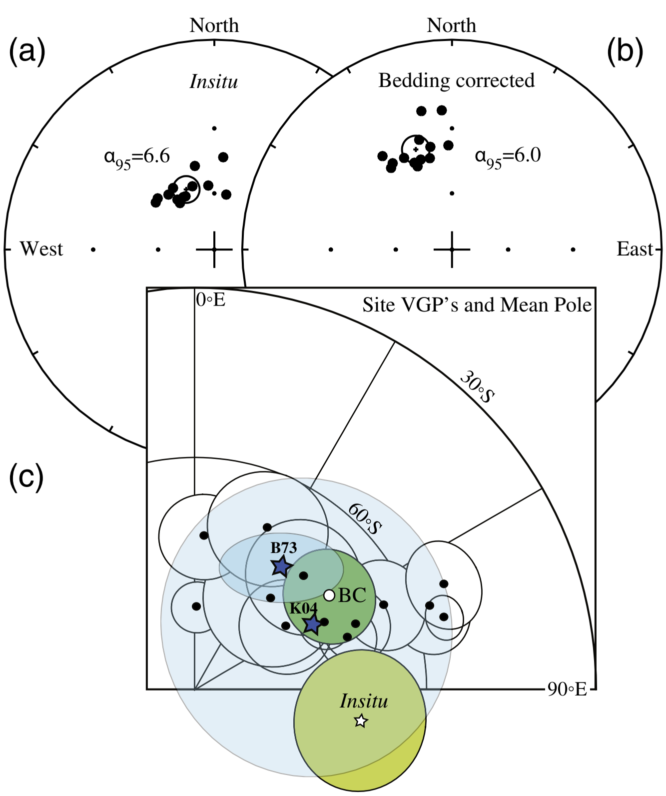

Fig. 4. Equal area plots of mean directions (a) before (in situ) and (b) after bedding correction. Mean directions are shown with α_{95} confidence circles; site mean directions shown as solid circles. (c) Orthogonal plot of bedding-corrected VGPs for each site (solid circles), mean pole for all sites, bedding corrected (BC) and before correction (in situ). We also compare our mean pole with two previous studies (dark blue stars with blue transparent confidence ovals) from the Moroccan Meseta CAMP volcanics. B73 = Bardon et al. (1973); K04 = Knight et al. (2004). All confidence ovals are A_{95} circles except the B73 pole (dp/dm oval): see Tables 1 and 2 (entries 24–26) for data details. (For interpretation of the references to color in this figure legend, the reader is referred to the web version of this article.)

A bedding-tilt test is not statistically significant at the 95% confidence level due to low variation of bedding orientations, but bedding correction decreases the ChRM directional scatter, suggestive of a pre-tilt, and possible primary, magnetization (see also Section 5). We calculate a mean bedding corrected declination/inclination of 340.1°/36.2° ($\alpha_{95} = 6.0°$), and a virtual geomagnetic pole (VGP) of 69.2°S and 55.5°E ($A_{95} = 6.0$; averaging site VGPs in Table 1). We interpret that this Argana pole adequately averages geomagnetic secular variation: VGPs are Fisher-distributed and the resulting geomagnetic dispersion S_F and bootstrapped 95% uncertainty bounds ($N = 13$, $S_F = 11.4°^{13.9°}_{8.2°}$) match those recorded in large CAMP dykes from Iberia and Morocco (Palencia-Ortas et al., 2010) and the global trend of the dispersion curve estimated for Jurassic lavas (Biggin et al., 2008). Finally, the A_{95} of 6.0 coincides with the lower limit of the reliability envelope of Deenen et al. (2011b), suggesting that the obtained scatter represents PSV. The Argana basalt geomagnetic dispersion is lower than that observed from CAMP lava flows in the High Atlas (Knight et al., 2004). The palaeomagnetic data in the latter study, however, were clustered in five 'directional groups', and probably leading to an overestimation of VGP scatter. Despite the fact that no "directional groups" have been observed in this study, within-section comparisons and site-mean directions of consecutive flows have been tested using the statistics of McFadden and Lowes (1981) for common true mean directions. Results indicate that sharing a common true mean direction cannot be discarded at the 95% confidence level only between sites BAR1–BAR2, BAR3–BAR4, and BAR5–BAR6. Combining these three couples (N = 10) leads to differences of less than 1° from those calculated with all the 13 sites, without significant changes in the statistical power.

5. Analysis

The uncorrected (in situ) Argana pole (Table 1) lies far from Jurassic to recent GAPWaP running mean poles in northwest Africa co-ordinates, therefore we discard a hypothetical post-tilt remagnetization origin. In contrast, the bedding corrected Argana pole (Table 1) matches well, despite the pioneering palaeomagnetic techniques or large uncertainties involved, with previous palaeomagnetic poles reported from CAMP lava flows in the Moroccan Meseta (e.g., Bardon et al., 1973; Knight et al., 2004; Fig. 4c, Table 2). It also lies very close to the global 200 Ma mean pole of Torsvik et al. (2008a) (Fig. 5a). We therefore conclude that the magnetic signature of the Argana basaltic flows is of primary nature.

We now proceed to compare our new Argana CAMP pole (ARG in Fig. 5a) with poles derived from the Messejana Plasencia (MePl in Fig. 5a) CAMP dykes in Iberia (Ortas et al., 2006), and the Ighrem and Foum Zguid (IGH + FZ in Fig. 5a) CAMP dykes in NW Africa east of the Atlas mountains (Palencia-Ortas et al., 2010). We discard recent magnetostratigraphic results by Deenen et al. (2011a) and Font et al. (2011), because these contained evidence for post-CAMP remagnetization or no test of secular variation averaging, and mean VGP calculated from sample-based mean directions. The ~200 Ma poles from these three plates (without any reconstructions) overlap at the 95% confidence level and suggest very minor *net-movements* since 200 Ma of both Iberia and the Moroccan Meseta with respect to NW Africa — obviously, we cannot assume that Iberia has remained fixed with respect to NW Africa since 200 Ma because of the large continental overlap with Newfoundland at the conjugate margin after adjusting for the opening history of the Central Atlantic; therefore alternative fits within the resolution power of the palaeomagnetic data are explored.

5.1. Iberia's location relative to NW Africa at 200 Ma

The position of Iberia with respect to North America and Europe has been studied for decades (e.g. Carey, 1958; Olivet, 1996; Osete et al.,

Table 2
A global 190–200 Ma palaeomagnetic compilation. Q = quality factor (Van der Voo, 1990, 1993); α_{95} = 95% confidence oval (or A_{95} if bold and underlined); C = comments: I = inclination corrected using the inclination–elongation (I/E) method of Tauxe and Kent (2004) or the anisotropy of magnetic susceptibility information (Kodama, 2009); # = corrected for counterclockwise Colorado Plateau rotation of 5.4° (Bryan and Gordon, 1990). Lat/Lon = pole latitude/longitude; CLat/CLon = pole latitude/longitude corrected for inclination shallowing with a flattening factor (f) of 0.6 (only for detrital sediments; sediment entries without a CLat/CLon are carbonates); RLat/RLon = pole rotated to NW Africa co-ordinates.

No	Q	α_{95}	Formation	Lat	Lon	CLat	CLon	RLat	RLon	Plate	Age (Ma)	C	GPDB refno/reference
1	5	3.1	Combined dykes	−72.8	268.1			−67.6	75.0	North America	190		1932
2	4	3	Liassic sediments	−77.0	315.0			−53.9	92.5	Europe	192		1467
3	4	6.2	Freetown Complex	−82.9	32.7			−82.9	32.7	NW Africa	193		3287
4	4	6.9	Storm Peak lavas	−44.1	231.5			−76.4	86.0	E Antarctica	193		808
5	5	8.9	Piedmont dykes	−66.0	266.0			−67.8	58.7	North America	194		1796
6	5	3.8	Vestfjella lavas and dykes	−41.8	226.5			−74.9	102.4	E Antarctica	195		1154
7	6	4.5	Mendoza sediments and volcanics	−51.0	223.0			−83.2	−33.6	Colorado (SAM)	195		Iglesia-Llanos et al. (2006)
8	5	3.8	Anari and Tapirapua Formations	−65.5	250.3			−70.7	27.4	Amazonia	197		3316
9	5	4	Hartford Newark basalts/volcanics	−68.0	268.5			−66.7	64.6	North America	197		2278
10	4	11.1	Connecticut Valley volcanics	−65.5	267.5			−67.0	58.2	North America	197		477
11	4	2.3	Newark volcanics	−63.0	263.1			−68.5	51.1	North America	197		1702
12	6	2.8	#Moenave Formation	−62.5	251.0			−74.0	48.2	North America	197	#, I	Donohoo-Hurley et al. (2010)
13	5	6.2	Watchung basalts	−63.6	268.7			−66.2	53.6	North America	197		1339
14	5	6	Hettangian Newark red beds	−55.6	274.6	−59.8	273.3	−63.0	46.7	North America	198		2312
15	5	7.5	Kerforne dykes	−61.0	259.0			−77.7	83.2	Europe	198		2743
16	5	**4**	French Guyana dykes	−81.2	235.1			−64.9	68.6	Amazonia	198		3378
17	5	7.9	Piedmont dykes	−61.5	234.0			−82.0	48.9	North America	199		1809
18	6	10.7	North Mountain basalt	−66.4	252.0			−73.2	62.1	North America	200		1932
19	5	4.1	Ighrem and Foum Zguid dykes	−73.0	64.7			−73.0	64.7	NW Africa	200		Palencia-Ortas et al. (2011)
20	7	3.2	Hartford basin	−66.6	268.2			−66.7	61.5	North America	201	I	Kent and Olsen (2008)
21	6	9	Hettangian–Sinemurian limestone	−55.0	280.0			−69.9	47.9	Europe	201		3141
22	7	3	Paris Basin sediments	−51.0	285.0			−66.3	38.6	Europe	201		3029
23	5	**3.5**	Messejana Plasencia dykes	−70.4	57.6			−68.8	61.6	Iberia	201		Ortas et al. (2006)
24	5	**6**	Argana Flows	−69.2	55.5			−69.2	55.5	Mor. Meseta	201		This study
25	3	7	Morrocan intrusives	−71.0	36.0			−71.0	36.0	Mor. Meseta	201		Bardon et al. (1973)
26	5	**19.1**	Central Atlantic Magmatic Province	−73.2	61.8			−73.2	61.8	Mor. Meseta	201		Knight et al. (2004)
27	4	4.9	Bolivar dykes, Venezuela	−66.9	245.6			−72.2	33.1	Amazonia	203		150
28	6	6.5	Newark Martinsville core	−64.9	276.6			−63.0	59.0	North America	204	I	Tan et al. (2007)
29	6	4.2	Chinle Formation, Redonda Member	−57.8	259.3	−59.6	259.5	−69.5	41.7	North America	204		152
30	6	10.7	Chinle Formation	−58.7	250.9	−62.8	251.2	−73.9	50.2	North America	204	#	2800
31	6	5	Newark Martinsville core	−67.8	275.8			−63.8	65.3	North America	204	I	Kent and Tauxe (2005)
32	5	8	Chinle Group	−58.5	256.9	−61.2	257.1	−71.0	45.4	North America	204		2979
33	6	4.5	Andesites, Ukraine	−50.0	286.4			−65.7	36.3	Europe	204		Yuan et al. (2011)
34	6	2.6	Zarzaitine Formation	−70.9	55.1	−76.2	78.9	−76.2	78.9	NW Africa	207		2932
35	3	5.9	Isalo Group	−74.0	97.1	−65.2	70.8	−51.7	56.1	Madagascar	207		147
36	5	4.6	Pachmarhi beds	−10.1	130.1	−2.4	118.5	−46.2	68.5	India	207		593
37	6	2.5	Newark Weston core	−58.1	271.8			−63.0	43.6	North America	207	I	Tan et al. (2007)
38	6	5	Newark Westonville	−66.9	267.2			−67.0	62.8	North America	207	I	Kent and Tauxe (2005)
39	6	8	Rhaetian sediments	−50.0	292.0	−58.0	272.9	−74.7	58.8	Europe	208		3141
40	6	5	Gipsdalen/Fleming Fjord Formations	−52.7	278.7			−68.1	30.5	Greenland	209	I	Kent and Tauxe (2005)
			Global mean (N = 40 poles)										
		2.7	NW Africa co-ordinates					−70.1	56.7	NW Africa	200 ± 10		

2011; Roest and Srivastava, 1991; Savostin et al., 1986; Sibuet et al., 2004; 2007; Srivastava and Verhoef, 1992; Srivastava et al., 2000; Van der Voo, 1969; Vissers and Meijer, 2012). Two competing models exist. The first infers that Iberia moved along a major left-lateral Cretaceous strike-slip zone to its current position, opening the Bay of Biscay in its wake (Olivet, 1996; Savostin et al., 1986), associated with only minor (~20°) counterclockwise Iberian rotation relative to Eurasia. The second model (Sibuet et al., 2004, 2007; Srivastava et al., 2000; Vissers and Meijer, 2012) infers a rifting stage, followed by a much larger (~40°) Albian–Aptian (Gong et al., 2008) rotation stage, which seems to be better supported by marine magnetic anomalies and the geological history of the Pyrenees (Vissers and Meijer, 2012). We note that Iberian position at 200 Ma following the 'strike-slip' model for opening of the Bay of Biscay (Olivet, 1996; Savostin et al., 1986) results in a very large and *statistically significant misfit* with the NW Africa CAMP pole (IGH + FZ dykes pole in Fig. 5b) if used in combination with the Central Atlantic fit of Labails et al. (2010), and only produces ~20° Cretaceous counterclockwise Iberian rotation instead of the ~40° measured palaeomagnetically (Gong et al., 2008; Osete et al., 2011; Vissers and Meijer, 2012). Conversely, if we use younger M0 (~120 Ma) to 175 Ma fits between Iberia and North America of Srivastava and Verhoef (1992), and the models derived from that (e.g. Osete et al., 2011; Sibuet et al., 2004, 2007; Vissers and Meijer, 2012) and recalculate the Iberia motion relative to NW Africa we obtain much better fits of the palaeomagnetic data, both for 200 Ma Iberia–Africa fits as well as for the Cretaceous counterclockwise rotation phase (Fig. 5c). We have therefore opted to maintain the 175 Ma fit of Iberia versus NW Africa (Table 3) by combining Labails et al.'s (2010) and Srivastava and Verhoef's (1992) rotations at 200 Ma; this results in a very tight fit of Iberia with Europe (Fig. 6a).

5.2. Tectonic stability of the Moroccan Meseta

The net shortening scenario of Sahabi et al. (2004) is possible within the palaeomagnetic resolution power but leads to larger dispersion of the 200 Ma CAMP poles (compare IGH–FZ dykes and ARG flows poles in Fig. 5a and b). A negligible *net-motion* scenario that seems to follow from geological constraints, as pointed out above, is favored from palaeomagnetic data and we therefore keep the Moroccan Meseta fixed to NW Africa at 200 Ma in our global reconstruction outlined below.

6. Earth at 200 Ma

6.1. A new global 200 Ma mean pole

Using the Argana pole previously described, the new CAMP Ighrem and Foum Zguid dyke pole from NW Africa (Palencia-Ortas

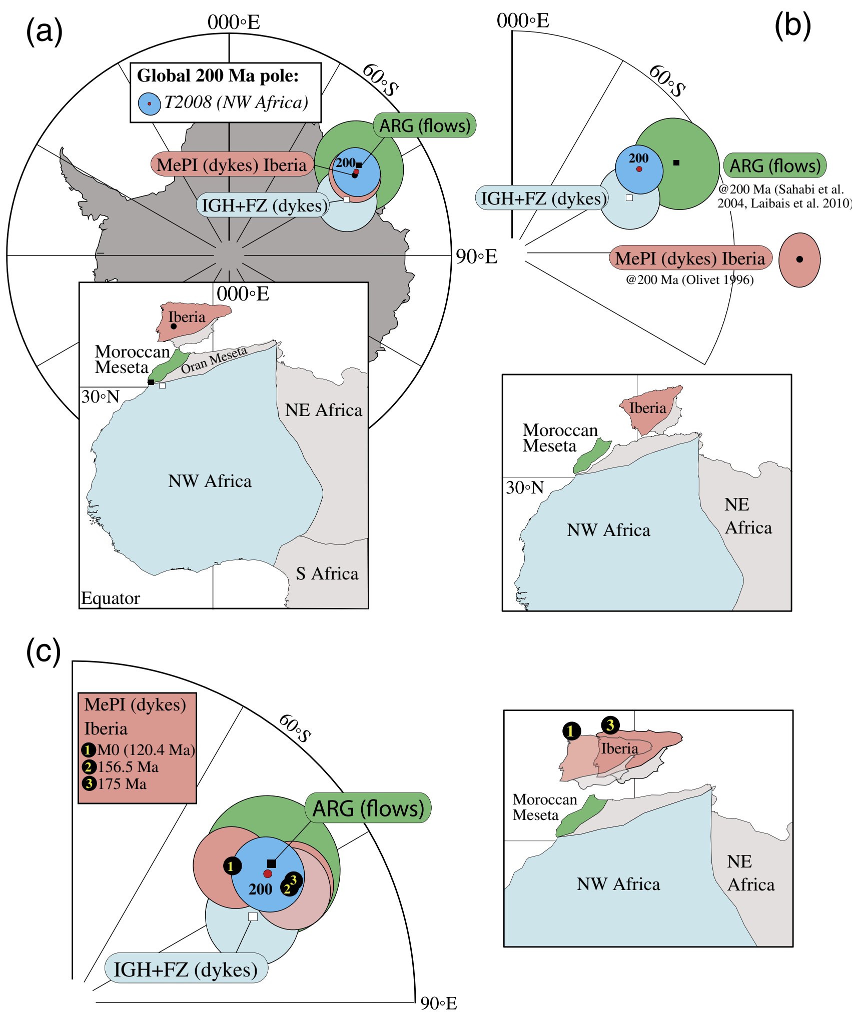

Fig. 5. (a) Comparison of a newly reported ~200 Ma palaeomagnetic pole from NW Africa [IGH + FZ (dykes); Palencia-Ortas et al., 2011], the ARG flows (this study) from the Moroccan Meseta, and ~200 Ma dykes from Iberia [MePI (dykes); Ortas et al., 2006]. All poles are derived from CAMP-related rocks and they are all shown in their local (original) reference frame. The global 200 Ma pole of Torsvik et al. (2008a) is shown in NW African co-ordinates with 95% confidence circle (A_{95}). Note how well all the ~200 Ma poles matches *without* making any relative corrections for Iberia vs. NW Africa and Moroccan Meseta vs. NW Africa (inset lower diagram). (b) The Moroccan Meseta ARG flow pole (this study) rotated to NW Africa co-ordinates, first interpolated from a ~195 Ma Euler pole of Sahabi et al. (2004; closure minimum) and the ~210 Ma Euler pole of Labails et al. (2010; closure maximum) for North America vs. Moroccan Meseta, and subsequently rotated to NW Africa [resulting Euler pole: Moroccan Meseta vs. NW Africa: lat. = 29.5° N; long. = 12.1° W, angle = 5.1°]. Similarly the MePI dyke pole from Iberia was first rotated to North America using the 200 Ma Euler pole of Olivet (1996; lat. = 75.4° N; long. = 8.0° W, angle = −46.2°). The resulting Euler pole of Iberia vs. NW Africa is lat. = 50.0° N; long. = 3.0° W and angle = 33.2°. Note the much larger dispersion of palaeomagnetic poles, notably for Iberia, which become statistically different from the two other poles, when using this Euler poles. The resulting continental fits using these Euler poles (in a NW Africa fixed reference frame) is shown in the lower inset diagram. (c) In this plot we maintain no correction for Moroccan Meseta vs. NW Africa while the Iberian palaeomagnetic pole is shown in three different fits: (1) M0 (120.4 Ma): lat. = 50.7° N; long. = 6.9° E and angle = −3.6° (calculated from Sibuet et al., 2004; following Srivastava et al., 2000 for Iberia vs. North America and Iberia vs. Europe), (2) 156.5 Ma Euler pole: lat. = 76.2° N; long. = 57.1° W and angle = 7.5° (calculated from Srivastava et al., 2000 for Iberia vs. North America), and (3) 175 Ma Euler pole: lat. = 67.6° N; long. = 41.7° W and angle = 5.6°. All these options are better than the Olivet (1996) 200 Ma fit. Orthogonal south polar projections. The resultant and preferred Jurassic–Early Cretaceous fits for a fixed Iberia vs. Europe or NW Africa are listed in Table 3.

et al., 2010) and the Messejana Plasencia pole from Iberia (Ortas et al., 2006; using the 200 Ma fit in Table 3), we calculate a new global 200 Ma pole based on palaeopoles and relative plate circuits listed in Tables 2–4. In addition to these three poles, our compilation differs from Torsvik et al. (2008a) as follows: (1) seven 'old' sedimentary poles are corrected for inclination (I) error (marked I in Table 2) using the inclination–elongation (Tauxe and Kent, 2004) or the anisotropy of magnetic susceptibility method (Kodama, 2009), (2) eight detrital sedimentary poles have been corrected for potential I-error using a benchmark flattening factor (*f*) of 0.6 (see Domeier et al., 2011; Torsvik et al., in review), and (3) a new Late Triassic (Norian) pole reported from Ukrainian andesites (Yuan et al., 2011).

The new global mean pole (N = 40), listed in NW African (Moroccan Meseta) co-ordinates (latitude = 70.1° S, longitude = 56.7° E), is almost

Table 3
Iberia versus a fixed Europe (EUR) or NW Africa (NWA). Lat/Long = Euler pole latitude/longitude.

Age	Lat	Long	Angle	EUR/NWA	Reference/comment
120.4	43.85	−5.83	−44.76	EUR	Sibuet et al. (2004) (after Srivastava et al., 2000)
122.0	43.60	−6.40	−44.75	EUR	After Sibuet et al. (2004)
156.5	43.85	−2.83	−44.76	EUR	Modified after Sibuet et al. (2004)
175.0	47.69	−0.01	−52.06	EUR	Recalculated to EUR from Srivastava and Verhoef (1992)
175.0	67.6	−41.7	5.6	NWA	Crossover: as above recalculated to NWA to maintain same fit back to 200 Ma
200.0	67.6	−41.7	5.6	NWA	See above

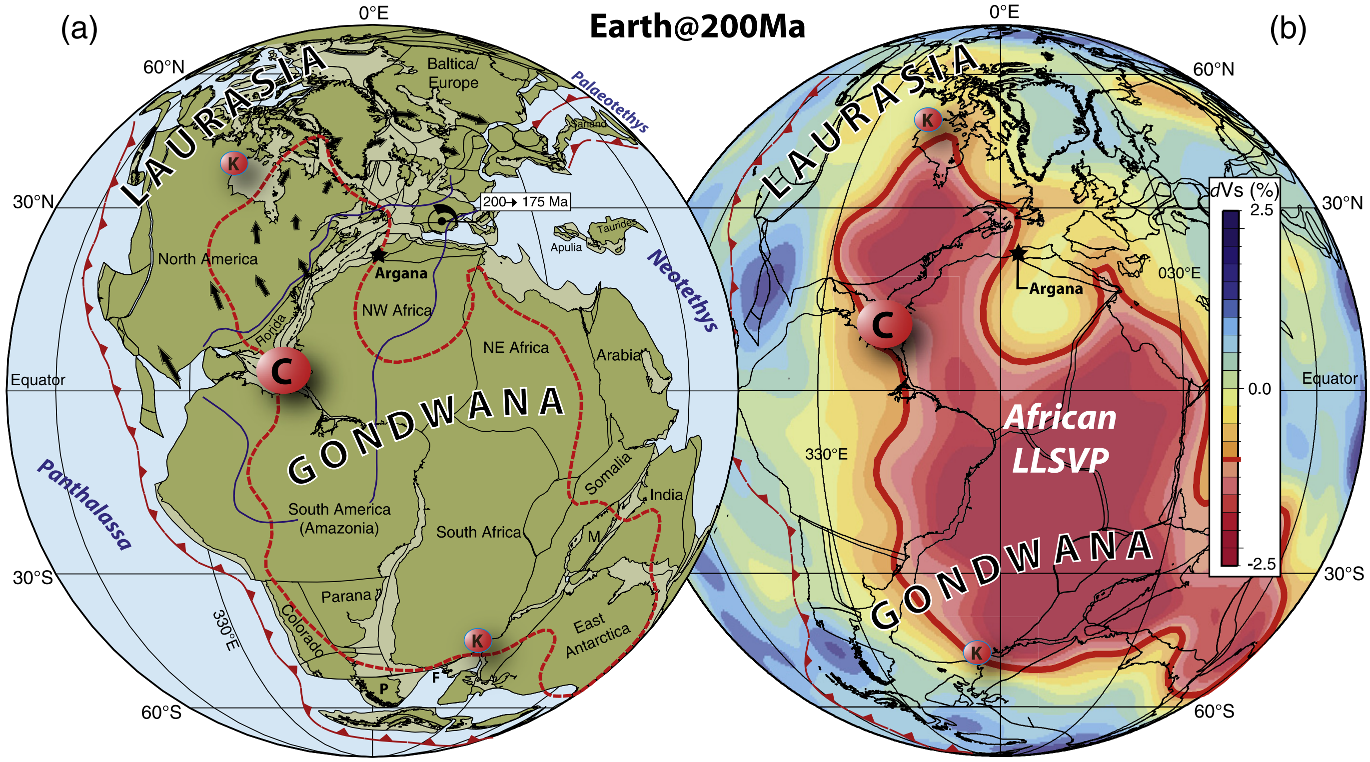

Fig. 6. (a) Palaeomagnetic reconstruction at ~200 Ma (mean global pole in NW African co-ordinates is 70.1° S and 56.7° E; $A_{95}=2.7°$; see Table 4 for relative plate circuits). Velocity fields (black arrows) for Laurasia are Pangean breakup vectors (190–185 Ma) relative to a fixed Gondwana (including Iberia). Laurasia is rotating clockwise around an Euler pole in SE Iberia until ~175 Ma. The Argana flows were located at 20.3° N ± 4.1° at eruption time. Possible outline/extent of CAMP related magmatism (thick dark blue line) simplified from McHone (2002). C = estimated plume center for the Central Atlantic Magmatic Province (CAMP), near the southern tip of Florida. Thick red stippled line is the 1% slow contour in (b). K = kimberlite occurrences at ~200 Ma in Southern Africa (Swaziland) and 196.2 Ma in North America (Rankin Inlet; Heaman and Kjarsgaard, 2000). Stippled black line in the Central Atlantic domain is the approximate plate boundary at breakup. P = Patagonia; F = Falklands; M = Madagascar. (b) Same reconstruction as in (a), but corrected for true polar wander (TPW), and draped on the SMEAN tomography model of Becker and Boschi (2002) near the core–mantle boundary (thick red line is the 1% slow contour in this model). The TPW corrected reconstruction (based on a mean pole of 50.7° S, 78.3° E and $A_{95}=2.7°$; NW African frame) is a so-called hybrid TPW-corrected palaeomagnetic reconstruction (Steinberger and Torsvik, 2008; Torsvik et al., 2008a), but here updated from Doubrovine et al. (in review) and Torsvik et al. (in review). (For interpretation of the references to color in this figure legend, the reader is referred to the web version of this article.)

identical to the Torsvik et al. (2008a) mean pole (but with reduced dispersion: A_{95} reduced from 3.2 to 2.7°), and *less than one degree* (GCD = 0.98°) *different from the Argana pole* (now included in the global mean pole calculation).

Table 4
Preferred plate circuits at ~200 Ma relative to a fixed NW Africa (/Moroccan Meseta). Relative fits are the same as for 250 Ma (Torsvik et al., in review), except those listed in brackets [] for North America, Iberia and Europe. SAM, South America.

Continent/plate	Euler latitude	Euler longitude	Euler angle
North America	64.3	−15.04	77.41
	[64.28]	[−14.74]	[78.05]
Iberia	67.6	−41.7	5.6
	[42.62]	[129.92]	[2.01]
Europe	48.69	0.27	60.54
	[46.79]	[3.19]	[56.02]
Moroccan Meseta	0	0	0
NE Africa	40.86	11.08	−2.69
Arabia	36.57	19.1	−11.18
South Africa	33.65	26.02	−2.34
Somalia	35.56	32.03	−2.29
Madagascar	18.99	129.77	−15.45
India	29.83	41.67	−62.74
Amazonia (SAM)	50.77	−35.13	53.46
Parana (SAM)	48.2	−35.83	54.6
Colorado (SAM)	48.2	−35.77	55.7
Patagonia (SAM)	48.22	−35.51	61.39
East Antarctica	10.93	146.47	−57.65
Australia	19.73	115.33	−56.84

6.2. Palaeogeography at 200 Ma

Pangea was drifting northward (8 cm/yr on average) while undergoing systematic counterclockwise rotations during the Triassic. NW Africa and the Moroccan Meseta moved ~13° northward during this interval and the CAMP-related Argana flows erupted at 20.3° N (±4.1°) at the dawn of the Jurassic. Our 250 (Fig. 1a) and 200 Ma (Fig. 6a) maps show many similarities but also important differences: Pangea was essentially equatorially centered and stretching from pole-to-pole but during the Triassic most of the Palaeotethys had been subducted at the expense of the widening Neotethys (Fig. 6a). For the Gondwanan core continents we maintain the same relative fits during the Triassic and we treat the Moroccan Meseta block as part of NW Africa, considering the Triassic rifting in the High Atlas (Frizon de Lamotte et al., 2008) as minor and therefore insignificant in applying relative corrections (see Section 5). We have implemented some pre-drift extension between Laurasia and Gondwana in the Late Triassic because of the formation of complex rift systems such as the Newark, Hartford, Deerfield and Fundy basins in eastern North America (e.g., Cirilli et al., 2009; Kent and Olsen, 2008; Weems and Olsen, 1997). Between Iberia and NW Africa/Moroccan Meseta we also invoke some Triassic extension (not detailed here but 200 and 250 Ma relative fits are listed in Table 4). Within Laurasia, between "Stable Europe" and Greenland/North America (NE Atlantic) we also invoke some extension there from the Late Triassic to the Early Jurassic (220–190 Ma; Torsvik et al., 2008a, in review). Pre-drift Triassic extensional corrections in some areas, however, can be rather small and thus hard to detect in our maps (Figs. 1 and 6a).

Continental breakup is often guided by pre-existing rheological heterogeneities. In the Central Atlantic case, pre-drift extension and sedimentary basin systems partly exploited lithospheric heterogeneities inherited from previous 'Wilson Cycles', i.e. Appalachian/Caledonian (Iapetus) and Alleghenian/Hercynian (Rheic) sutures (e.g., Thomas, 2006). Final breakup, however, and the opening of the Central Atlantic Ocean at ~195 Ma (Labails et al., 2010; Sahabi et al., 2004), occurred shortly (~6 Ma) after a massive episode of volcanism and CAMP formation (~201 Ma) as in many examples worldwide (e.g., Burke and Dewey, 1973). The CAMP plume head is commonly considered to have impinged the lithosphere somewhere beneath the southern tip of Florida (Fig. 6a, "Button C", thick blue line). Florida was a former peri-Gondwanan terrane, and it is significant that Central Atlantic breakup in this region occurred south rather than north of Florida, i.e. not along the upper Carboniferous–Permian Alleghenian suture as seen in the northeastern parts of the Central Atlantic opening system; this probably attests to the significance of the location of the CAMP plume head. The CAMP, however, extends over a vast area, more than 10 million km^2 (e.g., McHone, 2002) and the CAMP magma, if related to a single plume head (Fig. 6), must have propagated horizontally along the base of the lithosphere for several thousands of kilometers (see also Marzoli et al., 1999) — and to places, such as rifts that existed or were active in eastern North America, Morocco, Portugal/Spain and even France (e.g., Kerforne dykes in Brittany; Jourdan et al., 2003), where the lithosphere was already thin (Sleep, 1997).

The opening of the Central Atlantic symbolizes the main fragmentation of Pangea. In our model that closely follows Labails et al. (2010), the initial separation of Laurasia and Gondwana (minus Florida and some ex-Peri-Gondwanan elements) about an Euler pole located in SE Iberia (Fig. 6a) was rather slow (0.6 → 1.9 cm/yr between 200 and 175 Ma), but accelerated after 175 Ma with a peak velocity of 3.4 cm/yr at 155 Ma (M25).

6.3. Mantle–lithosphere interactions at 200 Ma

The origin of intra-plate volcanism such as CAMP is controversial, but a deep mantle plume origin is commonly assumed (Morgan, 1972). There are alternative models (e.g., Foulger et al., 2005), but Burke and Torsvik (2004), Burke et al. (2008) and Torsvik et al. (2006, 2008a,b, 2010) provide compelling evidence that plumes that generate LIPs and kimberlites rise from the margins of the long-lived Pacific and African Large Low Shear-wave Velocity Provinces (LLSVPs, Garnero et al., 2007) on the core–mantle boundary (CMB). In the SMEAN tomographic model (Becker and Boschi, 2002), the 1% slow contour (~2800 km depth) near the CMB is a good proxy for the plume generation zones (PGZs, Burke et al., 2008) at the edges of the LLSVPs.

Correlating surface LIPs and kimberlites with deep mantle heterogeneities (LLSVPs) require absolute plate reconstructions, but before the Cretaceous, only palaeomagnetic reconstructions are at hand. Palaeomagnetic reconstructions constrain latitudes (and rotations) but not longitudes, however an analytical ploy — selecting a reference plate that has remained stationary (or quasi-stationary) with respect to longitude, i.e. Africa (Burke and Torsvik, 2004), minimizes longitudinal worries. In Fig. 6a, Pangea is reconstructed according to the global 200 Ma palaeomagnetic pole, we use Africa as the reference plate and other continents are partnering in the plate circuit. We notice right away that not only the reconstructed CAMP plume head, but also contemporaneous kimberlites in southern Africa (Swaziland) and North America (Canada), plot vertically above the African PGZ. This correlation effectively demonstrates that (1) the African LLSVP has been stable for at least 200 Ma (and probably much longer, Torsvik et al., 2010), and (2) the CAMP (and the kimberlites) erupted above plumes that rose from the CMB.

Ideally, palaeomagnetic reconstructions should be corrected for true polar wander (TPW) because the LLSVPs are kept fixed in these correlative exercises. The TPW corrected reconstruction (Fig. 6b), however, based on the method of Steinberger and Torsvik (2008) and Torsvik et al. (in review), shows many similarities with Fig. 6a. Palaeomagnetic reconstructions – corrected or not corrected for TPW – show a striking correlation between CAMP and the PGZ. This is because of cumulative TPW since Pangea assembly is small, due to both clockwise and counter clockwise rotations centered near the mass-centers of the African/Pacific LLSVPs (Steinberger and Torsvik, 2008, 2010). Before TPW correction (Fig. 6a), we find that CAMP and kimberlite provinces in southern Africa and Canada plot at a distance of 2.5° to 12.6° (mean 8.4°) from the PGZ. After TPW correction (Fig. 6b) all these igneous bodies plot within 6° from the PGZ (mean 3.3°).

7. Conclusions

1. Palaeomagnetic data from the ~200 Ma CAMP-related Argana lavas (Morocco) are of excellent quality, the magnetic signature is considered primary and carried by Ti-poor titanomagnetites. Tilt-corrected data (declination = 340.1°, inclination = 36.2° and α_{95} = 6.0°) yield a palaeomagnetic pole (latitude = 69.2° S, longitude = 55.5° E and A_{95} = 6.0) that compares favorably with existing palaeomagnetic data from the Moroccan Meseta.
2. The Argana pole also compares well with CAMP-derived poles from both Iberia and NW Africa and implies very minor net-movements since 200 Ma of both Iberia and the Moroccan Meseta with respect to NW Africa. We therefore keep the Moroccan Meseta fixed to NW Africa in line with geological evidence while estimating an Euler pole fit of latitude = 67.6° N and longitude = 41.7° W (rotation angle = 5.6°) between Iberia and NW Africa. This Iberia–NW Africa fit is maintained from the early opening phase of the Central Atlantic until ~175 Ma.
3. Based on the above and a global compilation of palaeomagnetic poles between 190 and 210 Ma, we calculate a new global 200 Ma pole at latitude = 70.1° S, longitude = 56.7° E (A_{95} = 2.7°) in NW African co-ordinates. This mean pole is based on 40 poles and detrital sedimentary poles are corrected for I-error using the inclination–elongation/anisotropy of magnetic susceptibility methods, or corrected for potential I-error using a flattening factor of 0.6 when none of these methods were available.
4. From the global 200 Ma mean pole and our relative plate circuits we have constructed a new global map at this very important time in Earth history where Pangea is centered around the equator.
5. The CAMP plume head was impinging on the lithosphere at the equator at eruption time, and on our map, irrespective if we correct or not for true polar wander, there is a prominent correlation between the estimated CAMP plume head location and the plume generation zones at the core–mantle boundary.
6. Deep mantle plumes explain the surface distribution of CAMP and kimberlites in southern Africa and Canada at ~200 Ma, and the CAMP volcanism was likely to have been instrumental in the ensuing opening of the Central Atlantic (~195 Ma) and the consequent demise of Pangea.
7. Pangea breakup led to the separation of Laurasia and Gondwana at around an Euler pole located in SE Iberia. We considered Iberia's position linked to Gondwana during the initial breakup that must have been accompanied by ~100 km extension between Europe and Iberia, but some of this extension (within the resolution power of palaeomagnetic data) could have been accommodated between Iberia and Gondwana.

Acknowledgments

We are grateful for financial support from European Economic Area 'Abel Extraordinary Chairs' (NILS mobility grant); PR27/05-13936-BSCH and CGL2009-10840 (DGES) Spanish projects; Statoil (Akademiavtalen) and the European Research Council under the European Union's Seventh Framework Programme (FP7/2007–2013)/ERC

Advanced Grant Agreement Number 267631 (Beyond Plate Tectonics). We thank the geological guidance and help of Juan José Villalaín (UBU, Burgos) and Alicia Palencia-Ortas (ML-UCM, Madrid) during fieldwork. We thank Robin Cocks (The Natural History Museum, London) for comments. VCRM thanks the people at Physics of Geological Processes in Oslo for their hospitality during his NILS mobility stay in 2010. We thank C. Mac Niocaill and R. Van der Voo for their constructive reviews.

Appendix A. Supplementary data

Supplementary data to this article can be found online at doi:10.1016/j.epsl.2012.03.008.

References

Aït Chayeb, E.H., Youbi, N., El-Boukhari, A., Bouabdelli, M., Amrhar, M., 1998. Le volcanisme permien et mésozoïque inférieur du bassin d'Argana (Haut-Atlas occidental, Maroc): un magmatisme intraplaque associé à l'ouverture de l'Atlantique central. J. Afr. Earth Sci. 26 (4), 499–519 (in French).

Arboleya, M.-L., Teixell, A., Charroud, M., Julivert, M., 2004. A structural transect through the High and Middle Atlas of Morocco. J. Afr. Earth Sci. 39, 319–327.

Bardon, C., Bossert, A., Hamzeh, R., Westphal, M., 1973. Etude paléomagnétique de formations du Trias et du Jurassique du Maroc et du Sahara. CR Acad. Sci. Paris 276, 2357–2360 (in French).

Beauchamp, W., Allmendinger, R.W., Barazangi, M., Demnati, A., El Alji, M., Dahmani, M., 1999. Inversion tectonics and the evolution of the High Atlas Mountains, Morocco, based on a geological–geophysical transect. Tectonics 18, 163–184.

Becker, T.W., Boschi, L., 2002. A comparison of tomographic and geodynamic mantle models. Geochem. Geophys. Geosyst. 3 10.129/2001GC000168.

Besse, J., Courtillot, V., 2002. Apparent and true polar wander and the geometry of the geomagnetic field over the last 200 Myr. J. Geophys. Res. Solid Earth 107 (B11), 2300 doi: 1029/2000JB000050.

Biggin, A.J., Van Hinsbergen, D.J.J., Langereis, C.G., Straathof, G.B., Deenen, M.H.L., 2008. Geomagnetic secular variation in the Cretaceous Normal Superchron and in the Jurassic. Phys. Earth Planet. Inter. 169, 3–19. doi:10.1016/j.pepi.2008.07.004.

Brede, R., 1992. Structural aspects of the Middle and High Atlas (Morocco), phenomena and causalities. Geol. Rundsch. 81, 171–184.

Brown, R.H., 1980. Triassic rocks of Argana Valley, Southern Morocco, and their regional structural implications. Am. Assoc. Pet. Geol. Bull. 64, 988–1003.

Bryan, P., Gordon, R.G., 1990. Rotation of the Colorado Plateau: an updated analysis of paleomagnetic data. Geophys. Res. Lett. 17, 1501–1504. doi:10.1029/GL017i010p01501.

Burke, K., Dewey, J.F., 1973. Plume-generated triple junctions — key indicators in applying plate tectonics to old rocks. J. Geol. 81, 406–433.

Burke, K., Torsvik, T.H., 2004. Derivation of Large Igneous Provinces of the past 200 million -years from long-term heterogeneities in the deep mantle. Earth Planet. Sci. Lett. 227, 531–538.

Burke, K., Steinberger, B., Torsvik, T.H., Smethurst, M.A., 2008. Plume generation zones at the margins of Large Low Shear Velocity Provinces on the core–mantle boundary. Earth Planet. Sci. Lett. 265, 49–60.

Carey, S.W., 1958. A tectonic approach to continental drift. In: Carey, S.W. (Ed.), Continental Drift. A Symposium, Hobart, Tasmania.

Cirilli, S., Marzoli, A., Tanner, L., Bertrand, H., Buratti, N., Jourdan, F., Bellieni, G., Kontak, F., Renne, P.R., 2009. Latest Triassic onset of the Central Atlantic Magmatic Province (CAMP) volcanism in the Fundy Basin (Nova Scotia): new stratigraphic constraints. Earth Planet. Sci. Lett. 286, 514–525.

Cocks, L.R.M., Torsvik, T.H., 2011. The Palaeozoic geography of Laurentia and western Laurussia: a stable craton with mobile margins. Earth Sci. Rev. 106, 1–51. doi:10.1016/j.earscirev.2011.01.007.

Courtillot, V., Jaupart, C., Manighetti, I., Tapponnier, P., Besse, J., 1999. On causal links between flood basalts and continental breakup. Earth Planet. Sci. Lett. 166, 177–195.

Deenen, M.H.L., Ruhl, M., Bonis, N.R., Krijgsman, W., Kuerschner, W.M., Reitsma, M., van Bergen, M.J., 2010. A new chronology for the end-Triassic mass extinction. Earth Planet. Sci. Lett. 291, 113–125.

Deenen, M.H., Langereis, C.G., Krijgsman, W., El Hachimi, H., Chellai, E.H., 2011a. Palaeomagnetic results from Upper Triassic red beds and CAMP lavas of the Argana basin, Morocco. In: Van Hinsbergen, D.J.J., Buiter, S.J.H., Torsvik, T.H., Gaina, C., Webb, S.J. (Eds.), The Formation and Evolution of Africa: A Synopsis of 3.8 Ga of Earth History: Geological Society, London, Special Publication, 357, pp. 195–209. Doi: 10.1144/SP357.10.

Deenen, M.H.L., Langereis, C.G., van Hinsbergen, D.J.J., Biggin, A.J., 2011b. Geomagnetic secular variation and the statistics of paleomagnetic directions. Geophys. J. Int. 186, 509–520.

Dewey, J.F., Helman, M.L., Knott, S.D., Turco, E., Hutton, D.H.W., 1989. Kinematics of the western Mediterranean. In: Coward, M.P., Dietrich, D., Park, R.G. (Eds.), Alpine Tectonics: Geological Society, London, Special Publication, 45, pp. 265–283.

Domeier, M., Van der Voo, R., Torsvik, T.H., 2011. Paleomagnetism and Pangea: the road to reconciliation. Tectonophysics. doi:10.1016/j.tecto.2011.10.021.

Donohoo-Hurley, L.L., Geissman, J.W., Lucas, S.G., 2010. Magnetostratigraphy of the uppermost Triassic and lowermost Jurassic Moenave Formation, western United States: correlation with strata in the United Kingdom, Morocco, Turkey, Italy and the eastern United States. Geol. Soc. Am. Bull. 122, 1936–1950.

Doubrovine, P.V., Steinberger, B. And Torsvik, T.H., in review. Absolute plate motions in a reference frame defined by moving hotspots in the Pacific, Atlantic and Indian Oceans. J. Geophys. Res.

Dunlop, D.J., 2002. Theory and application of the Day plot (Mrs/Ms versus Hcr/Hc). 1. Theoretical curves and tests using titanomagnetite data. J. Geophys. Res. 107 (B3), 2056. doi:10.1029/2001JB000486.

El Hachimi, H., Youbi, N., Madeira, J., Bensalah, M.K., Martins, L., Mata, J., Medina, F., Bertrand, H., Marzoli, A., Munhá, J., Bellieni, G., Mahmoudi, A., Arbou, M.B., Assafar, H., 2011. Morphology, internal architecture and emplacement mechanisms of lava flows from the Central Atlantic Magmatic Province (CAMP) of Argana Basin (Morocco). In: Van Hinsbergen, D.J.J., Buiter, S.J.H., Torsvik, T.H., Gaina, C., Webb, S.J. (Eds.), The Formation and Evolution of Africa: A Synopsis of 3.8 Ga of Earth History: Geological Society, London, Special Publications, 357, pp. 167–193. Doi: 10.1144/SP357.9.

Fisher, R.A., 1953. Dispersion on a sphere. Proc. R. Soc. Lond. A Math. Phys. Sci. 217, 295–305.

Font, E., Youbi, N., Fernandes, S., El Hachimi, H., Kratinová, Z., Hamim, Y., 2011. Revisiting the magnetostratigraphy of the Central Atlantic Magmatic Province (CAMP) in Morocco. Earth Planet. Sci. Lett. 309, 302–317. doi:10.1016/j.epsl.2011.07.007.

Plates, plumes and paradigms. In: Foulger, G.R., Natland, J.H., Presnall, E., Anderson, D.I. (Eds.), Geological Society of America Special Paper, 288. 881 pp.

Frizon de Lamotte, D., Zizi, M., Missenard, Y., Hafid, M., El Azzouzi, M., Maury, R.C., Charriere, A., Taki, Z., Benammi, M., Michard, A., 2008. The Atlas system. In: Michard, A., Saddiqi, O., Chalouan, A., Frizon de Lamotte, D. (Eds.), Continental Evolution: The Geology of Morocco. : Lecture Notes in Earth Sciences, 116. Springer-Verlag, Berlin–Heidelberg, pp. 133–202.

Garnero, E.J., Lay, T., McNamara, A., 2007. Implications of lower-mantle structural heterogeneity for existence and nature of whole-mantle plumes. In: Foulger, G.R., Jurdy, D.M. (Eds.), Plates, Plumes, and Planetary Processes: Geological Society of America Special Paper, 430, pp. 79–101.

Gomez, F., Allmendinger, R.W., Barazangi, M., Er-Raji, A., Dahmani, M., 1998. Crustal shortening and vertical strain partitioning in the Middle Atlas Mountains of Morocco. Tectonics 17, 520–533.

Gong, Z., Langereis, C.G., Mullender, T.A.T., 2008. The rotation of Iberia during the Aptian and the opening of the Bay of Biscay. Earth Planet. Sci. Lett. 273, 80–93.

Heaman, L.M., Kjarsgaard, B.A., 2000. Timing of eastern North American kimberlite magmatism: continental extension of the Great Meteor hotspot track? Earth Planet. Sci. Lett. 178, 253–268.

Hesselbo, S.P., Robinson, S.A., Surlyk, F., Piasecki, S., 2002. Terrestrial and marine extinction at the Triassic–Jurassic boundary synchronized with major carbon-cycle perturbation: a link to initiation of massive volcanism? Geology 30, 251–254.

Iglesia-Llanos, M.P., Riccardi, A.C., Singer, S.E., 2006. Paleomagnetic study of Lower Jurassic marine strata from the Neuquén Basin, Argentina: a new Jurassic apparent polar wander path for South America. Earth Planet. Sci. Lett. 252, 379–397.

Johnson, C.L., Constable, C.G., Tauxe, L., Barendregt, R., Brown, L.L., Coe, R.S., Layer, P., Mejia, V., Opdyke, N.D., Singer, B.S., Staudigel, H., Stone, D.B., 2008. Recent investigations of the 0–5 Ma geomagnetic field recorded by lava flows. Geochem. Geophys. Geosyst. 9, Q04032 doi: 10.1029.2007GC001696.

Jourdan, F., Marzoli, A., Bertrand, H., Cosca, M., Fontignie, D., 2003. The northernmost CAMP: $^{40}Ar/^{39}Ar$ age, petrology and Sr–Nd–Pb isotope geochemistry of the Kerforne Dike, Brittany, France. In: Hames, W.E., McHone, J.G., Renne, P.R., Ruppel, C. (Eds.), The Central Atlantic Magmatic Province: Insights from Fragments of Pangea, AGU Geophys. Mon, 136.

Kent, D.V., Irving, E., 2010. Influence of inclination error in sedimentary rocks on the Triassic and Jurassic apparent pole wander path for North America and implications for Cordilleran tectonics. J. Geophys. Res. B: Solid Earth 115 (10) art. no. B10103.

Kent, D.V., Olsen, P.E., 2008. Early Jurassic magnetostratigraphy and paleolatitudes from the Hartford continental rift basin (eastern North America): Testing for polarity bias and abrupt polar wander in association with the central Atlantic magmatic province. J. Geophys. Res. 113, B06105. doi:10.1029/2007JB005407.

Kent, D.V., Tauxe, L., 2005. Corrected Late Triassic latitudes for continents adjacent to the North Atlantic. Science 307, 240–244.

Kirschvink, J.L., 1980. The least-square line and plane and the analysis of paleomagnetic data. Geophys. J. Roy. Astron. Soc. 62, 699–718.

Klitgord, K.D., Schouten, H., 1986. Plate kinematics of the Central Atlantic. In: Vogt, P.R., Tucholke, B.E. (Eds.), The Geology of North America: The Western North Atlantic Region, vol. M. Geological Society of America, Boulder, Colorado, pp. 351–378.

Knight, K.B., Nomade, S., Renne, P.R., Marzoli, A., Betrand, H., Youbi, N., 2004. The Central Atlantic Magmatic Province at the Triassic–Jurassic boundary: paleomagnetic and $^{40}Ar/^{30}Ar$ evidence from Morocco for brief, episodic volcanism. Earth Planet. Sci. Lett. 228, 143–160.

Kodama, K.P., 2009. Simplification of the anisotropy-based inclination correction technique for magnetite- and hematite bearing rocks: a case study for the Carboniferous Glenshaw and Mauch Chunk formations, North America. Geophys. J. Int. 176, 467–477.

Labails, C., Roest, W.R., 2010. Comments on “Breakup of Pangaea and plate kinematics of the central Atlantic and Atlas regions” by Schettino and Turco (2009). Geophys. J. Int. 183, 96–98.

Labails, C., Olivet, J.L., Aslanian, D., Roest, W.R., 2010. An alternative early opening scenario for the Central Atlantic Ocean. Earth Planet. Sci. Lett. 297, 355–368.

Manspeizer, W., Puffer, J.H., Cousminer, H.L., 1978. Separation of Morocco and eastern North America: a Triassic–Liassic stratigraphic record. Geol. Soc. Am. Bull. 89, 901–920.

Marzoli, A., Renne, P.R., Piccirillo, E.M., Ernesto, M., Bellieni, G., De Min, A., 1999. Extensive 200-million-year-old continental flood basalts of the Central Atlantic magmatic province. Science 284, 616–618.

Marzoli, A., Bertrand, H., Knight, K.B., Cirilli, S., Buratti, N., Vérati, C., Nomade, S., Renne, P.R., Youbi, N., Martini, R., Allenbach, K., Neuwerth, R., Rapaille, C., Zaninetti, L., Bellieni, G.,

2004. Synchrony of the Central Atlantic magmatic province and the Triassic–Jurassic boundary climatic and biotic crisis. Geology 32, 973–976.
Matte, P., 2001. The Variscan collage and orogeny (480–290 Ma) and the tectonic definition of the Armorica microplate: a review. Terra Nova 13, 122–128.
McFadden, P.L., Lowes, F.J., 1981. The discrimination of mean directions drawn from Fisher distributions. Geophys. J. R. Astron. Soc. 67, 19–33.
McHone, J.G., 2002. Volatile emissions of Central Atlantic Magmatic Province basalts: mass assumptions and environmental consequences. In: Hames, W.E., McHone, J.G., Renne, P.R., Ruppel, C. (Eds.), The Central Atlantic Magmatic Province: American Geophysical Union, Geophysical Monograph, 136, pp. 241–254.
Medina, F., 1991. Superimposed extensional tectonics in the Argana Triassic formations (Morocco), related to the early rifting of the Central Atlantic. Geol. Mag. 128, 525–536.
Morgan, W.J., 1972. Deep mantle convection plumes and plate motions. Bull. Am. Assoc. Pet. Geol. 56, 203–213.
Nomade, S., Knight, K.B., Beutel, E., Renne, P.R., Verati, C., Féraud, G., Marzoli, A., Youbi, N., Bertrand, H., 2007. Chronology of the Central Atlantic Magmatic Province: implications for the Central Atlantic rifting processes and the Triassic–Jurassic biotic crisis. Paleogeogr. Paleoclimatol. Paleoecol. 244, 326–344. doi:10.1016/j.paleo.2006.06.034.
Olivet, J.L., 1996. La cinématique de la plaque Ibérique. Bull. Centres Rech. Explor.-Prod. Elf-Aquitaine 20, 191–195 (in French).
Olsen, P.E., Kent, D.V., Et-Touhami, M., Puffer, J.H., 2003. Cyclo-, magneto-, and bio-stratigraphic constraints on the duration of the CAMP event and its relationship to the Triassic–Jurassic boundary. In: Hames, W.E., McHone, J.G., Renne, P.R., Ruppel, C. (Eds.), The Central Atlantic Magmatic Province: Insights From Fragments of Pangea: Geophysical Monograph Series, 136, pp. 7–32.
Ortas, A., Osete, M.L., Vegas, R., Silva, P., 2006. Paleomagnetic study of the Messejana Plasencia dyke (Portugal and Spain): a lower Jurassic paleopole for the Iberian plate. Tectonophysics 420, 455–472.
Osete, M.L., Gómez, J.J., Pavón-Carrasco, F.J., Villalaín, J.J., Palencia-Ortas, A., Ruiz-Martínez, V.C., Heller, F., 2011. The evolution of Iberia during the Jurassic from palaeomagnetic data. Tectonophysics 502, 105–120. doi:10.1016/j.tecto.2010.05.025.
Palencia-Ortas, A., Ruiz. Martínez, V.C., Osete, M.L., 2010. Analysis of the Jurassic geomagnetic dispersion recorded by the Iberian magmatism and preliminary paleomagnetic data of Jurassic volcanic rocks from the southeast Iberian Ranges. Fis. Tierra 22, 35–58 (in Spanish).
Palencia-Ortas, A., Ruiz-Martínez, V.C., Villalaín, J.J., Osete, M.L., Vegas, R., Touil, A., Hafid, A., McIntosh, G., van Hinsbergen, D.J.J., Torsvik, T.H., 2011. A new 200 Ma paleomagnetic pole for Africa, and paleo-secular variation scatter from Central Atlantic Magmatic Province (CAMP) intrusives in Morocco (Ighrem and Foum Zguid dykes). Geophys. J. Int. 185, 1220–1234. doi:10.1111/j.1365-246X.2011.05017.x.
Roest, W.R., Srivastava, S., 1991. Kinematics of the plate boundaries between Eurasia, Iberia and Africa in the North Atlantic from the late Cretaceous to the present. Geology 19, 613–616.
Ruhl, M., Deenen, M.H., Abels, H.A., Bonis, N.R., Krijgsman, W., Kürschner, W.M., 2010. Astronomical constraints on the duration of the early Jurassic Hettangian stage and recovery rates following the end-Triassic mass extinction (St Audrie's Bay/East Quantoxhead, UK). Earth Planet. Sci. Lett. 295, 262–276.
Ruiz-Martínez, V.C., Villalaín, J.J., Palencia-Ortas, A., Ruiz-Martínez, V.C., Villalaín, J.J., Palencia-Ortas, A., 2007. Paleomagnetic and AMS results of Late Triassic red beds, CAMP-related lava flows and Lower Jurassic limestones from Argana Basin, Morocco: geodynamic implications. Our Changing Planet. Proceedings of IUGG XXIV General Assembly Perugia, Italy 2007 (IAGA ASI002 Symposium 'Paleomagnetism and Geodynamics Neotectonics, Continental Reconstruction, Reference frames', 3047), Compiled by L. Ubertini, P. Manciola, S. Casadei, S. Grimaldi, 68http://www.iugg2007perugia.it/webbook/pdf/A.pdf.
Sahabi, M., Aslanian, D., Olivet, J.-L., 2004. Un nouveau point de départ pour l'histoire de l'Atlantique central. CR Geosci. 336, 1041–1052.
Savostin, L.A., Sibuet, J.C., Zonenshain, L.P., Le Pichon, X., Roulet, M.-J., 1986. Kinematic evolution of the Tethys belt from the Atlantic Ocean to the Pamirs since the Triassic. Tectonophysics 123, 1–35.
Schettino, A., Scotese, C.R., 2005. Apparent polar wander paths for the major continents (200 Ma to the present day): a paleomagnetic reference frame for global plate tectonic reconstructions. Geophys. J. Int. 163, 727–759.
Schettino, A., Turco, E., 2009. Breakup of Pangaea and plate kinematics of the central Atlantic and Atlas regions. Geophys. J. Int. 178, 1078–1097.
Schoene, B., Crowley, J.L., Condon, D.C., Schmitz, M.D., Bowring, S.A., 2006. Reassessing the uranium decay constants for geochronology using ID-TIMS U–Pb data. Geochim. Cosmochim. Acta 70, 426–445. doi:10.1016/j.gca.2005.09.007.
Schoene, B., Bartolini, A., Schaltegger, U., Blackburn, T.J., 2010. Correlating the end-Triassic mass extinction and flood basalt volcanism at the 100 ka level. Geology 38–5, 387–390. doi:10.1130/G30683.1.
Şengör, A.M.C., Yilmaz, Y., Sungurlu, O., 1984. Tectonics of the Mediterranean Cimmerides: nature and evolution of the western termination of Paleo-Tethys. Geol. Soc. Lond. Spec. Publ. 17, 77–112.
Sibuet, J.C., Srivastava, S.P., Spakman, W., 2004. Pyrenean orogeny and plate kinematics. J. Geophys. Res. 109, B08104 doi: 08110.01029/02003JB002514.
Sibuet, J.-C., Srivastava, S.P., Manatschal, G., 2007. Exhumed mantle-forming transitional crust in the Newfoundland–Iberia rift and associated magnetic anomalies. J. Geophys. Res. 112, B06105. doi:10.1029/2005JB003856.
Sleep, N.H., 1997. Lateral flow and ponding of starting plume material. J. Geophys. Res. 102 (B5), 10001–10012 doi: 0148-0227/97/97JB-00551.
Srivastava, S.P., Verhoef, J., 1992. Evolution of Mesozoic sedimentary basins around the North Central Atlantic: a preliminary plate kinematics solution. In: Parnell, J. (Ed.), Basins on the Atlantic seaboard: Petroleum Geology, Sedimentology and Basin Evolution. Geological Society, London, pp. 397–420.
Srivastava, S.P., Sibuet, J.C., Cande, S., Roest, W.R., Reid, I.D., 2000. Magnetic evidence for slow seafloor spreading during the formation of the Newfoundland and Iberian margins. Earth Planet. Sci. Lett. 182, 61–76.
Stampfli, G.M., Borel, G.D., 2002. A plate tectonic model for the Paleozoic and Mesozoic constrained by dynamic plate boundaries and restored synthetic oceanic isochrons. Earth Planet. Sci. Lett. 196 (1–2), 17–33.
Steinberger, B., Torsvik, T.H., 2008. Absolute plate motions and true polar wander in the absence of hotspot tracks. Nature 452 (7187), 620–623.
Steinberger, B., Torsvik, T.H., 2010. Toward an explanation for the present and past locations of the poles. Geochem. Geophys. Geosyst. 11 Q06W06.
Tan, X.D., Kodama, K.P., Gilder, S., Courtillot, V., 2007. Rock magnetic evidence for inclination shallowing in the Passaic Formation red beds from the Newark basin and a systematic bias of the Late Triassic apparent polar wander path for North America. Earth Planet. Sci. Lett. 254, 345–357.
Tauxe, L., Kent, D.V., 2004. A simplified statistical model for the geomagnetic field and the detection of shallow bias in paleomagnetic inclinations: was the ancient magnetic field dipolar? In: Channell, J.E.T., Kent, D., Lowrie, W., Meert, J.G. (Eds.), Timescales of the Paleomagnetic Field. : Geophysical Monograph 145. AGU, Washington, DC, pp. 101–117.
Teixell, A., Arboleya, M.-L., Julivert, M., Charroud, M., 2003. Tectonic shortening and topography in the central High Atlas (Morocco). Tectonics 22, 1051. doi:10.1029/2002TC001460.
Thomas, W.A., 2006. Tectonic inheritance at a continental margin. GSA Today 16 (2), 4–11.
Torsvik, T.H., Cocks, L.R.M., 2004. Earth geography from 400 to 250 million years: a paleomagnetic, faunal and facies review. J. Geol. Soc. Lond. 161, 555–572.
Torsvik, T.H., Van der Voo, R., Preeden, U., Mac Niocaill, C., Steinberger, B., Doubrovine, P.V., van Hinsbergen, D.J.J., Domeier, M., Gaina, C., Tohver, E., Meert, J.G., McCausland, P.J., Cocks, R.L.R., in review. Phanerozoic polar wander, paleogeography and dynamics. Earth Sci. Rev.
Torsvik, T.H., Smethurst, M.A., Burke, K., Steinberger, B., 2006. Large igneous provinces generated from the margins of the large low-velocity provinces in the deep mantle. Geophys. J. Int. 167, 1447–1460. doi:10.1111/j.1365-246X.2006.03158.x.
Torsvik, T.H., Müller, R.D., Van der Voo, R., Steinberger, B., Gaina, C., 2008a. Global plate motion frames: Toward a unified model. Rev. Geophys. 46. doi:10.1029/2007RG000227 RG3004.
Torsvik, T.H., Steinberger, B., Cocks, L.R.M., Burke, K., 2008b. Longitude: linking Earth's ancient surface to its deep interior. Earth Planet. Sci. Lett. 276, 273–282.
Torsvik, T.H., Burke, K., Webb, S., Ashwal, L., Steinberger, B., 2010. Diamonds sampled by plumes from the core–mantle boundary. Nature 466, 352–355.
van der Meer, D.G., Spakman, W., van Hinsbergen, D.J.J., Amaru, M.L., Torsvik, T.H., 2010. Toward absolute plate motions constrained by lower mantle slab remnants. Nat. Geosci. 3, 36–40.
Van der Voo, R., 1969. Paleomagnetic evidence for the rotation of the Iberian Peninsula. Tectonophysics 7, 5–56.
Van der Voo, R., 1990. Phanerozoic paleomagnetic poles from Europe and North America and comparisons with continental reconstructions. Rev. Geophys. 28, 167206.
Van der Voo, R., 1993. Paleomagnetism of the Atlantic, Tethys and Iapetus Oceans. Cambridge University Press. 411 pp.
Verati, C., Rapaille, C., Feraud, G., Marzoli, A., Bertrand, H., Youbi, N., 2007. 40Ar/39Ar ages and duration of the Central Atlantic Magmatic Province volcanism in Morocco and Portugal and its relation to the Triassic–Jurassic boundary. Paleogeogr. Paleoclimatol. Paleoecol. 244, 308–325.
Vissers, R.L.M., Meijer, P.Th., 2012. Mesozoic rotation of Iberia: subduction in the Pyrenees? Earth Sci. Rev. 110, 93–110.
Weems, R.E., Olsen, P.E., 1997. Synthesis and revision of groups within the Newark Supergroup, eastern North America. N. Am. Geol. Soc. Am. Bull. 109, 195–209.
Wegener, A., 1915. Die Entstehung der Kontinente und Ozeane, 23. Samml. Vieweg, Braunschweig. 94 pp.
Westphal, M., Montigny, R., Thuizat, R., Bardon, C., Bossert, A., Hamzeh, R., Rolley, J.P., 1979. Paléomagnétisme et datation du volcanisme permien, triasique et crétacé du Maroc. Can. J. Earth Sci. 16, 2150–2164 (in French).
Whiteside, J.H., Olsen, P.E., Kent, D.V., Fowell, S.J., Et-Touhami, M., 2007. Synchrony between the Central Atlantic magmatic province and the Triassic–Jurassic mass-extinction event? Paleogeogr. Paleoclimatol. Paleoecol. 244, 345–367. doi:10.1016/j.paleo.2006.06.035.
Whiteside, J.H., Olsen, P.E., Eglinton, T., Brookfield, M.E., Sambrotto, R.N., 2010. Compound-specific carbon isotopes from Earth's largest flood basalt eruptions directly linked to the end-Triassic mass extinction. Proc. Natl. Acad. Sci. U. S. A. 107, 6721–6725.
Yuan, K., Van der Voo, R., Bazhenov, M.L., Bakhmutov, V., Alekhin, V., Hendriks, B.W.H., 2011. Permian and Triassic paleolatitudes of the Ukrainian shield with implications for Pangea reconstructions. Geophys. J. Int. 184, 595–610.